

On the Convergence of the Gradient Descent Method with Stochastic Fixed-Point Rounding Errors under the Polyak–Łojasiewicz Inequality

Lu Xia^{1*}, Stefano Massei² and Michiel E. Hochstenbach¹

^{1*}Department of Mathematics and Computer Science, Eindhoven University of Technology, Eindhoven, 5600 MB, The Netherlands.

²Department of Mathematics, Università di Pisa, Pisa, 56127, Italy.

*Corresponding author(s). E-mail(s): l.xia1@tue.nl;

Contributing authors: stefano.massei@unipi.it; m.e.hochstenbach@tue.nl;

Abstract

In the training of neural networks with low-precision computation and fixed-point arithmetic, rounding errors often cause stagnation or are detrimental to the convergence of the optimizers. This study provides insights into the choice of appropriate stochastic rounding strategies to mitigate the adverse impact of roundoff errors on the convergence of the gradient descent method, for problems satisfying the Polyak–Łojasiewicz inequality. Within this context, we show that a biased stochastic rounding strategy may be even beneficial in so far as it eliminates the vanishing gradient problem and forces the expected roundoff error in a descent direction. Furthermore, we obtain a bound on the convergence rate that is stricter than the one achieved by unbiased stochastic rounding. The theoretical analysis is validated by comparing the performances of various rounding strategies when optimizing several examples using low-precision fixed-point arithmetic.

Keywords: Fixed-point arithmetic, rounding error analysis, gradient descent, low-precision, stochastic rounding, Polyak–Łojasiewicz inequality

Mathematics Subject Classification: 97N20 , 62J02 , 65G30 , 65G50 , 68T01

1 Introduction

To reduce computing time and hardware complexity, low-precision numerical formats are becoming increasingly popular, especially in the area of machine learning. However, when training neural networks (NNs) using low-precision computation, rounding errors frequently result in stagnation or negatively affect the convergence of the optimizers.

Both floating-point and fixed-point arithmetics are commonly used in low-precision training [1–3]. Although the floating-point format has a wider number representation, owing to the non-uniform distributed number representation, considerable research efforts focus on improving both offline training and online inference with fixed-point representation. The latter is employed in power-efficient devices such as field-programmable gate arrays (FPGAs) and dedicated application-specific integrated circuits (ASICs). These practical low-cost embedded microprocessors and microcontrollers often rely on fixed-point arithmetic for finite-precision signal processing due to the cost and complexity of floating-point hardware. Additionally, low-precision fixed-point arithmetic is gaining increasing attention in AI-powered drone development; see, e.g., [4–6].

This work is concerned with the gradient descent method (GD), which is the method of choice for a large group of machine learning problems, in view of its computational efficiency and stable convergence. GD has a sublinear convergence for convex problems and it has been shown to have linear convergence for both strongly convex problems [7] and problems satisfying the *Polyak–Lojasiewicz inequality* (PL) [8–10]. Note that strongly convex functions also satisfy the PL condition; see [10, Appendix B]. The PL condition has been recently analyzed by [10] for optimization problems in machine learning, e.g., least squares and logistic regression. Also, a wide range of NNs satisfies the PL condition [11–13] and variants thereof [14].

In the context of low-precision training of NNs, the utilization of the classical *round to nearest method* (RN) [15, Sec. 2.3] may cause stagnation, while the employment of the unbiased stochastic rounding method, that we call *stochastic rounding* (SR) (see, e.g., [16, Sec. 3]), has been experimentally shown to provide training accuracy similar to single-precision computation; see, e.g., [1, 2, 17, 18]. Therefore, the choice of appropriate rounding methods plays a critical role in the training of NNs in low-precision computation. Given this, there is a growing demand to conduct a thorough error analysis that encompasses both deterministic and stochastic rounding errors throughout the entire gradient descent updating procedure. By gaining a deeper understanding of the factors contributing to the stagnation of GD in low-precision computation, we can make informed decisions in selecting an appropriate rounding method for training NNs.

Previous work. In our previous work [19], we have analyzed the influence of stochastic *floating-point* roundoff error on the convergence of GD in low-precision computation for *convex* problems. We have theoretically explained why SR can help prevent the stagnation of GD in the floating-point environment. Moreover, we have introduced two new stochastic rounding methods, namely ε -*biased stochastic rounding* (SR_ε) and *signed-SR* $_\varepsilon$ (see subsection 2.2 for a summary of these rounding methods); the latter are more effective than SR in speeding up the convergence of GD when employed for rounding the outcome of the floating-point operations encountered during

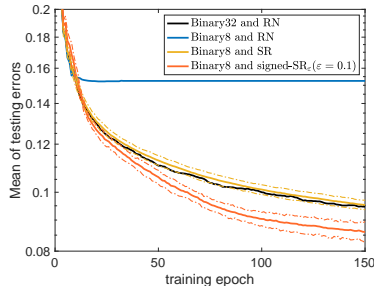


Fig. 1 Mean of testing errors of training a multinomial logistic regression model on the MNIST dataset over 20 simulations. The number representation systems and rounding strategies compared are: Binary32 with RN, Binary8 with RN, SR, and signed-SR $_{\epsilon}$. The dashed lines indicate the estimated 95% confidence intervals of the methods involving a stochastic rounding strategy.

the execution of the algorithm. As an example, Figure 1 shows the mean value of testing errors of training a multinomial logistic regression model (MLR) using different number representation systems, and rounding methods. The application of signed-SR $_{\epsilon}$ with an 8-bit number format (Binary8) [19, Sec. 2.1] dramatically accelerates the convergence of GD compared to that obtained by SR with Binary8 and RN with single-precision computation (Binary32). All operations in the MLR training are performed using the specified number formats, except for the softmax evaluations, which are first evaluated in double precision and then rounded to the specified number formats.

Contributions of the paper. We study the impact of the *fixed-point* rounding errors on the convergence of GD for problems satisfying the PL condition. Here the stagnation of the algorithm is caused by the absolute rounding errors, hence the analysis is significantly different from the one concerning the stagnation in the floating-point case. We demonstrate that the customized sign of the rounding bias, which has been the main motivation for introducing signed-SR $_{\epsilon}$ in [19], is not necessary in the case of fixed-point arithmetic. In particular, SR $_{\epsilon}$ and signed-SR $_{\epsilon}$ result in the same rounding bias when choosing the same ϵ . We prove that, for both SR and SR $_{\epsilon}$, the linear convergence rate of GD under the PL condition is preserved for low-precision fixed-point computations and that GD with SR $_{\epsilon}$ satisfies a stricter convergence bound than that of GD with SR. Finally, we compare the influence of fixed-point and floating-point rounding errors on the convergence of GD. The comparison illustrates that the implementation of GD using SR $_{\epsilon}$ with floating-point arithmetic performs similarly to a gradient descent method with automatically adapted stepsizes in each coordinate of the current iterate. On the other hand, the implementation using SR $_{\epsilon}$ with fixed-point arithmetic behaves like a combination of vanilla gradient descent and stochastic sign gradient descent methods.

Notations. We denote the Euclidean norm and infinity norm by $\|\cdot\|$ and $\|\cdot\|_{\infty}$, respectively. We indicate by $\mathbb{F} \subseteq \mathbb{R}$ the subset of the real numbers that are exactly representable within the chosen number representation system. Specifically, given a real number $x \in \mathbb{R}$ and a rounding method, $\tilde{x} \in \mathbb{F}$ is used to denote a corresponding fixed-point representation; this may be a result of a single rounding operation, or an accumulation of rounding errors (as in (5)). This quantity depends on the specific

rounding procedure, and is a random variable in the case of stochastic rounding. We denote by L the Lipschitz constant for the gradient of the objective function and by χ the largest distance between the iterates generated by GD and the minimizer, i.e., $\chi := \max_k \|\mathbf{x}^{(k)} - \mathbf{x}^*\| < \infty$, where $\mathbf{x}^{(k)} \in \mathbb{R}^n$; in particular, we assume that the iterates of GD remain in a compact set. Furthermore, the rounding precision, i.e., the distance between two subsequent fixed-point numbers, is indicated by u . For instance, in binary representation, the rounding precision in fixed-point arithmetic with one fractional point can be expressed as $u = 2^{-1}$. In the context of floating-point representations, u indicates the relative approximation error due to rounding, i.e., 2^{1-m} , where m is the number of bits employed for the mantissa. We employ \simeq and \lesssim to denote approximate equality and inequality with error bounded up to second and higher-order terms in u and a hidden constant with at most polynomial dependence on n , L , and χ .

1.1 Problem setting

Let us briefly recall the convergence behavior of GD for the problems with Lipschitz continuous gradients and satisfying the PL inequality. We consider an unconstrained optimization problem for a differentiable function f with a non-empty solution set

$$\mathcal{X}^* := \arg \min_{\mathbf{x} \in \mathbb{R}^n} f(\mathbf{x}),$$

and we denote the optimal value by $f^* := f(\mathbf{x}^*)$, for any $\mathbf{x}^* \in \mathcal{X}^*$, where f satisfies the following assumption.

Problem Assumption. Let $f : \mathbb{R}^n \rightarrow \mathbb{R}$ be a differentiable function whose gradient $\nabla f : \mathbb{R}^n \rightarrow \mathbb{R}^n$ is Lipschitz continuous with constant $L > 0$, that is:

$$\|\nabla f(\mathbf{x}) - \nabla f(\mathbf{y})\| \leq L \|\mathbf{x} - \mathbf{y}\|, \quad \text{for all } \mathbf{x}, \mathbf{y} \in \mathbb{R}^n. \quad (1)$$

In addition, f satisfies the PL inequality:

$$2\mu(f(\mathbf{x}) - f^*) \leq \|\nabla f(\mathbf{x})\|^2, \quad \text{for all } \mathbf{x} \in \mathbb{R}^n. \quad (2)$$

For quadratic functions $f(\mathbf{x}) = \frac{1}{2} \mathbf{x}^T A \mathbf{x}$, where A is symmetric positive definite, μ and L can be taken as the smallest and largest eigenvalue of A , respectively. For general twice continuously differentiable functions it holds that $\mu \leq L$, which we can see as follows. For this argument, we may assume without loss of generality that $f^* = 0$ and $\mathbf{0} \in \mathcal{X}^*$. Using the Taylor series at this point, we get

$$\mu \mathbf{x}^T \nabla^2 f(\mathbf{0}) \mathbf{x} + \mathcal{O}(\|\mathbf{x}\|^3) = 2\mu f(\mathbf{x}) \leq \|\nabla f(\mathbf{x})\|^2 \leq L^2 \|\mathbf{x}\|^2.$$

By taking \mathbf{x} in the direction of the largest eigenvalue of $\nabla^2 f(\mathbf{0})$ in modulus, we conclude $\mu \leq L$. Usually, μ will be considerably smaller than L . For the readability of our results, it turns out convenient to assume that $\mu \leq \frac{1}{2}L$; we have therefore added

this condition to our assumption (cf. Assumption 1 in subsection 3.2). We point out that this is not a restriction; slightly modified results hold without this extra clause. For instance, for some results instead of requiring the updating stepsize $t \leq \frac{1}{L}$, we need $t \leq \min\{\frac{1}{L}, \frac{1}{2\mu}\}$. Additionally, as explained in [10], (2) implies that every stationary point \mathbf{x}^* is a global minimum. Therefore, a unique globally optimal solution is not implied by our assumption. We remark that our statements hold with weaker hypotheses, for instance by requiring that (1) and (2) are only satisfied in a certain domain that contains all the iterates of GD.

In exact arithmetic, GD updates iteratively in the opposite direction of the gradient, given by

$$\mathbf{x}^{(k+1)} = \mathbf{x}^{(k)} - t \nabla f(\mathbf{x}^{(k)}), \quad (3)$$

where $t \in \mathbb{R}$ is the *stepsize*. When optimizing problems satisfying (1) and (2) using GD in exact arithmetic, a linear convergence rate is proven by [8]. A simple version of this proof is given by [10].

Theorem 1. [10, Thm. 1] *Let the objective function f satisfy (1) and (2). In exact arithmetic, the k th iteration step of the gradient descent method with a fixed stepsize $t \leq \frac{1}{L}$ satisfies the following inequality:*

$$f(\mathbf{x}^{(k)}) - f^* \leq (1 - t\mu)^k (f(\mathbf{x}^{(0)}) - f^*). \quad (4)$$

Throughout the paper, we assume that there is no overflow and, for convenience, we assume that both the stepsize t and the starting point $\mathbf{x}^{(0)}$ are fixed-point numbers, i.e., $t = \tilde{t}$ and $\mathbf{x}^{(0)} = \tilde{\mathbf{x}}^{(0)}$. Under these assumptions, there are two sources of roundoff errors at each iteration of GD, i.e., the absolute rounding errors caused by evaluating $\nabla f(\tilde{\mathbf{x}}^{(k)})$ at $\tilde{\mathbf{x}}^{(k)}$ and multiplying the evaluated gradient $\nabla f(\tilde{\mathbf{x}}^{(k)})$ by t in a limited precision; the latter are denoted by $\sigma_1^{(k)}$ and $\sigma_2^{(k)}$, respectively. Therefore, we can write the updating rule of GD with rounding errors as

$$\tilde{\mathbf{x}}^{(k+1)} = \tilde{\mathbf{x}}^{(k)} - t \nabla f(\tilde{\mathbf{x}}^{(k)}) - t \sigma_1^{(k)} - \sigma_2^{(k)}. \quad (5)$$

Comparing the implementation of GD in fixed-point arithmetic (5) to the exact arithmetic (3), the rounding errors $\sigma_1^{(k)}$ and $\sigma_2^{(k)}$ may affect the convergence speed and accuracy depending on the magnitude and sign of the absolute rounding errors.

We analyze the influence of rounding errors on the convergence of GD concerning two aspects of the method: monotonicity and convergence rate with respect to the objective function value. During the execution of GD, it is common to see differences in magnitudes among the various components of the gradient vector. To conduct a thorough error analysis throughout the entire updating procedure, we identify three cases depending on the relation between the magnitudes of the gradients and the rounding precision. In Case I, the updating vectors of GD consist entirely of scaled gradient components, i.e., $t |\nabla f(\tilde{\mathbf{x}}^{(k)})_i + \sigma_{1,i}^{(k)}| \geq u$ for all i . In the second case, the updating vectors of GD are on the level of the rounding errors, i.e., $t |\nabla f(\tilde{\mathbf{x}}^{(k)})_i + \sigma_{1,i}^{(k)}| < u$ for all i (Case II). In the last case (Case III), the updating vectors of GD depend on both the scaled gradient components and the rounding errors, i.e., some components of $t |\nabla f(\tilde{\mathbf{x}}^{(k)}) + \sigma_1^{(k)}|$ satisfy Case I and others fulfill Case II.

Among the three cases, Case I is the one that most likely describes the updating procedure of GD in the initial iteration steps when the starting point is far from the optimal point. Cases II and III apply to situations when the gradient has some or all components close to the rounding precision u . For all three cases, we assume that each coordinate of the gradient function is assessed with a *non-opposite sign* (cf. Definition 1) to their exact values. In particular, the non-opposite sign evaluation indicates that the component-wise multiplication of the rounded gradient and its exact value is always a non-negative vector. Therefore, the convergence of GD is proven to be guaranteed at least until each coordinate of the gradient function is close to the level of u , i.e., $\|\nabla f\| = \mathcal{O}(\sqrt{nu})$. We prove that in Case I, the employment of SR with low-precision computation leads to the same linear convergence bound, in expectation, as the exact computation for the problems satisfying the PL condition. For Cases II and III, the convergence bound of GD may be slightly larger than that for the exact computation. When SR_ε is employed, we prove that a stricter convergence bound is achieved compared to SR and may be even stricter than the bound applicable to the exact computation.

1.2 Main theoretical contributions

The main contribution of this study is to provide sufficient conditions to ensure linear convergence of GD with the presence of rounding errors. For ease of presentation, we display the bound of the convergence rate for the following case. We assume that the objective function f satisfying (1) and (2) is optimized using GD with fixed-point arithmetic; from the start to the k_1 th iteration the updating rule satisfies Case I, from the $(k_1 + 1)$ st to the k_2 th iteration it satisfies Case II, and from the $(k_2 + 1)$ st to the k_3 th iteration it satisfies Case III. Note that this assumed order of cases aims at simplifying the notation; cases may have different orders and the theoretical result applies to any order.

If both σ_1 and σ_2 in (5) are results of SR with fixed stepsize $t \leq \frac{1}{4L}$ and under the assumption that $\theta_{j_1} > 0$, where θ_{j_1} is defined in (33), as shown in Corollary 10 and Propositions 12 and 15, then with α_{j_2} as defined in (47) the convergence rate satisfies

$$\mathbb{E}[f(\tilde{\mathbf{x}}^{(k)}) - f^*] \lesssim (1 - \mu t)^{k_1} \prod_{j_1=k_1+1}^{k_2} (1 - \mu t \theta_{j_1}) \prod_{j_2=k_2+1}^{k_3} (1 - \mu(t + \alpha_{j_2}))(f(\mathbf{x}^{(0)}) - f^*),$$

where all the factors, apart from $f(\mathbf{x}^{(0)}) - f^*$, are in the interval $(0, 1)$.

If σ_1 is the result of SR and σ_2 is obtained using SR_ε in (5) with fixed stepsize $t \leq \frac{1}{4L}$ and under the assumption that $\theta_{j_1}, \theta_{j_2} > 0$, see Theorem 9 and Propositions 14 and 16, then with τ_1, τ_2 as defined in (27) and (43), respectively, the convergence rate satisfies

$$\begin{aligned} & \mathbb{E}[f(\tilde{\mathbf{x}}^{(k)}) - f^*] \\ & \lesssim (1 - \mu(t + \tau_1))^{k_1} \prod_{j_1=k_1+1}^{k_2} (1 - \mu \theta_{j_1}(t + \tau_2)) \prod_{j_2=k_2+1}^{k_3} (1 - \mu(t + \alpha_{j_2} + \theta_{j_2} \tau_2))(f(\mathbf{x}^{(0)}) - f^*), \end{aligned}$$

where all the factors, apart from $f(\mathbf{x}^{(0)}) - f^*$, are in the interval $(0, 1)$. In particular, the presence of the (positive) quantities τ_1 and τ_2 suggests faster convergence of GD when SR_ε is used instead of SR for rounding the multiplication between the gradient and the step size. Detailed discussions on τ_1 and τ_2 are provided in Propositions 14 and 16, respectively. We remark that instead of using a norm-wise assumption to guarantee the monotonicity of the algorithm, we employ the component-wise assumptions $\theta_{j_1}, \theta_{j_2} > 0$ that are sufficient but not necessary to achieve a linear convergence rate in different cases. On the other hand, the use of a norm-wise assumption on the gradient would result in a cumbersome analysis when targeting a linear convergence rate. Additionally, in the numerical study of section 6, we show examples where $\theta_{j_1}, \theta_{j_2}$ are negative, and GD suffers from stagnation using SR.

A summary of all the theoretical results with respect to different cases is given in Table 1. Note that we only consider the use of SR when evaluating gradients. The reason is that SR ensures an estimation of the gradient with a non-opposite sign compared to the exact arithmetic and this property is crucial for the theoretical analysis. In contrast, ensuring the latter property with SR_ε appears difficult in our setting.

Table 1 Summary of the theoretical results.

Case	Result	Rounding strategy	Reference
I	Convergence rate	General	Theorem 7
	Convergence rate	$\sigma_1(\text{SR})$ and $\sigma_2(\text{SR}_\varepsilon)$	Theorem 9
	Convergence rate	$\sigma_1(\text{SR})$ and $\sigma_2(\text{SR})$	Corollary 10
II	Monotonicity	$\sigma_1(\text{SR})$ and $\sigma_2(\text{SR})$	Proposition 11
	Convergence rate	$\sigma_1(\text{SR})$ and $\sigma_2(\text{SR})$	Proposition 12
	Monotonicity	$\sigma_1(\text{SR})$ and $\sigma_2(\text{SR}_\varepsilon)$	Proposition 13
	Convergence rate	$\sigma_1(\text{SR})$ and $\sigma_2(\text{SR}_\varepsilon)$	Proposition 14
III	Convergence rate	$\sigma_1(\text{SR})$ and $\sigma_2(\text{SR})$	Proposition 15
	Convergence rate	$\sigma_1(\text{SR})$ and $\sigma_2(\text{SR}_\varepsilon)$	Proposition 16

1.3 Outline of the paper

Section 2 reviews the basic properties of fixed-point arithmetic and the rounding rules that will be used in this paper. There, we identify the non-opposite sign property to guarantee the descent direction of rounding errors when implementing GD in low-precision computation. In section 3, the rounding errors are analyzed with respect to its sign and magnitude. Based on the magnitude of rounding errors, we categorize the updating vector of GD into the three cases that we already mentioned in subsection 1.1. In section 4, the impact of the rounding bias on the convergence of GD is studied for problems satisfying (1) and (2) in each of the three cases. Section 5 compares the influence of rounding bias on the convergence of GD in floating-point and fixed-point arithmetic. We validate our theoretical findings with several numerical simulations in section 6. Finally, conclusions are presented in section 7.

2 Number representation and rounding schemes

Let us introduce fixed-point arithmetic and review the definitions of different rounding methods: RN, SR, SR_ε , and signed- SR_ε . Then, we define the non-opposite sign property for the rounded values, which will be used to guarantee the descent direction in GD.

2.1 Fixed-point representation

Fixed-point arithmetic is an alternative way to represent numbers in low-cost embedded microprocessors and microcontrollers, where a floating-point unit is unavailable. Fixed-point numbers are mostly in base 2 (binary representation). We use the format $\text{Q}[\text{QI}].[\text{QF}]$ to represent binary fixed-point numbers and use the two's complement¹ for the sign, where QI denotes the number of integer bits and QF denotes the number of fractional bits [20]. For instance, a Q4.6 number presents a 10-bit value with 4 integer bits and 6 fractional bits. Moreover, the rounding precision is given by $u = 2^{-\text{QF}}$. The fixed-point arithmetic used in the numerical experiments is implemented using Matlab's `fi` toolbox.

2.2 Review of rounding methods

When converting a real number to a fixed-point number format, we denote by $\text{fi}(\cdot)$ a general rounding operator that maps $x \in \mathbb{R}$ to $\text{fi}(x) \in \mathbb{F}$. Throughout this study, we consider rounding schemes of the form

$$\text{fi}(x) = \begin{cases} \lfloor x \rfloor, & \text{with probability } p(x), \\ \lfloor x \rfloor + u, & \text{with probability } 1 - p(x), \end{cases} \quad (6)$$

with $p(x) \in [0, 1]$, and $\lfloor x \rfloor = \max\{y \in \mathbb{F} : y \leq x\}$ indicating the largest representable fixed-point number less than or equal to x . When a specific rounding scheme is applied, $\text{fi}(\cdot)$ and p are replaced by the corresponding rounding operator and probability, respectively. Specifically, we denote p_r , p_0 , p_ε , and $p_{\varepsilon s}$, the rounding probabilities of rounding to the nearest, unbiased stochastic rounding, ε -biased stochastic rounding, and signed ε -biased stochastic rounding, respectively.

Round to the nearest method with half to even (RN) is the default rounding mode applied in IEEE 754 floating-point operations. It forces the least significant bit (LSB) to 0 in the case of a tie [21]. When we use RN as the rounding operator ($\text{fi} = \text{RN}$) in (6), we have $p_r(x) = 1$ when $x - \lfloor x \rfloor < \frac{1}{2}u$ or when $x - \lfloor x \rfloor = \frac{1}{2}u$ and LSB of $\lfloor x \rfloor$ is even.

Unbiased stochastic rounding (SR) provides an unbiased rounded result by setting a probability that is proportional to the distance from x to the nearest representable fixed-point number. Some basic properties and the backward error analysis of SR have recently been studied by [16]. When SR is employed as the rounding operator

¹Adding a 1 to the least significant (rightmost) bit after inverting the bits of the absolute value.

(fi = SR) in (6), we have

$$p_0(x) = 1 - (x - \lfloor x \rfloor) / u. \quad (7)$$

ε -**biased stochastic rounding** (SR_ε) has been introduced by [19]. It provides a rounding bias with the same sign as its input by increasing or decreasing by $\varepsilon \in (0, 1)$ the probability of rounding down in SR, depending on the sign of the input number (cf. (8b)). When we choose SR_ε as the rounding operator (fi = SR_ε) in (6), we have

$$p_\varepsilon(x) := \varphi(\eta(x, \varepsilon)), \quad (8a)$$

with

$$\eta(x, \varepsilon) := 1 - (x - \lfloor x \rfloor) / u - \text{sign}(x) \varepsilon, \quad \varphi(y) = \begin{cases} 0, & y \leq 0, \\ y, & 0 \leq y \leq 1, \\ 1, & y \geq 1. \end{cases} \quad (8b)$$

Signed-SR $_\varepsilon$ is a variant of SR_ε where we can customize the sign of the rounding bias by replacing $\text{sign}(x)$ in (8b) with the sign of the additional variable $v \in \mathbb{R}$, i.e.,

$$p_{\varepsilon s}(x) := \varphi(\eta_s(x, \varepsilon, v)), \quad (9a)$$

with

$$\eta_s(x, \varepsilon, v) := 1 - (x - \lfloor x \rfloor) / u - \text{sign}(v) \varepsilon. \quad (9b)$$

A detailed description of SR_ε and signed- SR_ε , and their implementations, can be found in [19, Sec. 2.2]. We will use all four rounding methods for the convergence analysis in sections 4 and 5.

2.3 Preserving non-opposite sign of fixed-point arithmetic operations

Under the assumption that there is no overflow, the addition and subtraction of fixed-point numbers within the same number format are performed without introducing any rounding errors. However, representing the product of two fixed-point numbers may require more digits than those used for representing the factors [22]; e.g., multiplying two 8-bit values produces a 16-bit result, in general. In the case of multiplication, we adopt the following model to present the rounded value

$$\text{fi}(\tilde{x} \tilde{y}) = \tilde{x} \tilde{y} + \sigma, \quad \text{where} \begin{cases} |\sigma| < u & \text{for SR, SR}_\varepsilon \text{ and signed-SR}_\varepsilon, \\ |\sigma| \leq \frac{1}{2}u & \text{for RN,} \end{cases} \quad (10)$$

where $\text{fi} \in \{\text{RN}, \text{SR}, \text{SR}_\varepsilon, \text{signed-SR}_\varepsilon\}$ and $\text{fi}(\tilde{x} \tilde{y}) \in \{\lfloor \tilde{x} \tilde{y} \rfloor, \lfloor \tilde{x} \tilde{y} \rfloor + u\}$. The main difference between (10) and the model of floating-point computation [15, Sec. 2.1] is that

the rounding error σ is ensured to be small only in an absolute sense. Due to the rounding properties, we always have $\text{sign}(\text{fi}(\tilde{x}\tilde{y}))\text{sign}(\tilde{x}\tilde{y}) \geq 0$. Specifically, for a single operation, all the rounding schemes mentioned in subsection 2.2 will not result in a rounded value with an opposite sign as its input.

However, this may be different when a series of operations is implemented. For instance, using SR to compute $\text{fi}(0.24) - \text{fi}(0.26)$, by first rounding the two numerical values in the binary number format Q1.1 ($u = \frac{1}{2}$), and then evaluating their difference. We have

$$\text{SR}(0.24) - \text{SR}(0.26) = \begin{cases} 0.5, & \text{with probability } 0.2304, \\ 0, & \text{with probability } 0.4992, \\ -0.5, & \text{with probability } 0.2704. \end{cases}$$

Similar issues are encountered in deterministic rounding. Despite the monotonicity of RN, i.e., $x \leq y \in \mathbb{R}$ implies $\text{RN}(x) \leq \text{RN}(y)$, when more than two rounding errors are accumulated, an opposite sign may be obtained; for instance, within the number format Q1.1, we have

$$\text{sign}(\text{RN}(0.26) + \text{RN}(-0.24) + \text{RN}(-0.24)) = -\text{sign}(0.26 - 0.24 - 0.24).$$

In subsection 3.1, we will see that it is crucial to ensure that the rounded gradient preserves the sign of each component of the exact gradient, as this causes GD to update in a non-ascent direction. For this reason, we introduce the property of *non-opposite sign* for the rounded result obtained from a series of operations within a given number format.

Definition 1 (non-opposite sign). *When evaluating $g : \mathbb{R}^n \rightarrow \mathbb{R}$ in fixed-point arithmetic at $\tilde{\mathbf{x}} \in \mathbb{F}^n$, we say that the resulting value $\widetilde{g(\tilde{\mathbf{x}})}$ has the non-opposite sign property if*

$$\text{sign}(\widetilde{g(\tilde{\mathbf{x}})}) \text{sign}(g(\tilde{\mathbf{x}})) \geq 0.$$

To facilitate further analysis, we propose a condition to guarantee the non-opposite sign property for RN and stochastic rounding methods. Denote by σ_g the accumulated rounding error in evaluating $g(\tilde{\mathbf{x}})$, such that $\widetilde{g(\tilde{\mathbf{x}})} = g(\tilde{\mathbf{x}}) + \sigma_g$. If

$$|g(\tilde{\mathbf{x}})| \geq |\sigma_g|, \tag{11}$$

then it easily follows that $\widetilde{g(\tilde{\mathbf{x}})}$ has the non-opposite sign property.

Now, we analyze what happens in expectation to the sign of stochastically rounded quantities. In the case of SR, we demonstrate that the zero mean property implies the non-opposite sign in expectation when $g(\tilde{\mathbf{x}})$ can be evaluated using a finite sequence of elementary operations.

Proposition 2. *Let $g : \Gamma \rightarrow \mathbb{R}$, with $\Gamma \subseteq \mathbb{R}^n$ an open set, be a function that can be evaluated with a finite sequence of the elementary operations $(+, -, *, /)$, and let $\widetilde{g(\tilde{\mathbf{x}})}$ be the corresponding random variable obtained by evaluating the operations using*

fixed-point arithmetic and SR for rounding, at the point $\tilde{\mathbf{x}} \in \Gamma \cap \mathbb{F}^n$. If overflow and division by zero are not encountered, then

$$|\mathbb{E}[g(\tilde{\mathbf{x}})] - g(\tilde{\mathbf{x}})| \lesssim c u^2, \quad (12)$$

where c depends the number of multiplications and divisions performed for evaluating $g(\tilde{\mathbf{x}})$, and may depend on the point $\tilde{\mathbf{x}}$ itself.

Proof. Let σ_g denote the accumulated error caused by evaluating g so that $\widetilde{g(\tilde{\mathbf{x}})} = g(\tilde{\mathbf{x}}) + \sigma_g$. If the evaluation of $g(\tilde{\mathbf{x}})$ requires m elementary operations, then considering the Taylor expansion of the accumulated error, in accordance with [23, (8)], we have

$$\sigma_g = \sum_{i=1}^m c_{m,i} \sigma_i + \sum_{i=1}^m \sum_{j=1}^i c_{m,ij} \sigma_i \sigma_j + \mathcal{O}(u^3),$$

where σ_i and σ_j indicate the error introduced by single operations and $c_{m,i}, c_{m,ij}$ are certain scalar coefficients. The zero mean independence property for SR [16, Lemma 5.2] implies that $\mathbb{E}[\sigma_i] = 0$ and $\mathbb{E}[\sigma_i \sigma_j] = 0$ for $i \neq j$. Therefore, we achieve

$$|\mathbb{E}[\sigma_g]| \leq \sum_{i=1}^m |c_{m,ii}| \sigma_i^2 + \mathcal{O}(u^3) \leq c u^2 + \mathcal{O}(u^3),$$

where c is problem-dependent and can be obtained based on Table 1 in [23]. Note that Table 1 in [23] is based on floating-point arithmetic; when fixed-point arithmetic is applied, only the coefficients in multiplication and division operations are relevant. \square

Example 1. For instance, when $g(\tilde{\mathbf{x}}) = \tilde{x}_1^2 + \tilde{x}_1 \tilde{x}_2$, based on the Taylor expansion and Table 1 in [23], the accumulated error can be expressed as $\sigma_g = 2\tilde{x}_1 \sigma_{\tilde{x}_1} + \tilde{x}_2 \sigma_{\tilde{x}_1} + \tilde{x}_1 \sigma_{\tilde{x}_2} + \sigma_{\tilde{x}_1}^2 + \mathcal{O}(u^3)$, where the constant in front of $\sigma_{\tilde{x}_1}^2$ is obtained from the fifth row and column in Table 1 in [23]. Therefore, using SR, the expectation of the accumulated error is bounded by $\mathbb{E}[\sigma_g] \leq u^2$.

Therefore, when using SR, we have that $\mathbb{E}[\widetilde{g(\tilde{\mathbf{x}})}]$ has a non-opposite sign with respect to $g(\tilde{\mathbf{x}})$. However, this property cannot be guaranteed by SR_ε . In the next section, we analyze the influence of rounding errors on the convergence of GD under the PL condition for different rounding strategies on the basis of (11) and Proposition 2.

3 Gradient descent method with fixed-point arithmetic

Near an optimum, the GD algorithm in finite precision may move back and forth around the minimum repeatedly; see, e.g., [24, Fig. 9.2]. This zigzag behavior is generally caused by the rapid change in negative gradient direction and can be mitigated by reducing the stepsize (setting a smaller t) or adding a momentum term; see, e.g., the heavy ball method [25] and Nesterov's accelerated method [7, (2.2.11)]. Although reducing the stepsize mitigates the zigzag behavior, when implementing GD in low

precision and with RN, a small stepsize may prevent GD from converging because of the loss of gradient information. This issue is known as the vanishing gradient problem and can be overcome using stochastic rounding strategies [2, 19]. We start our convergence analysis by studying the role of rounding errors during the updating procedure of GD for fixed-point arithmetic.

A key tool for our analysis is the *update vector incorporating rounding errors* of GD (cf. (5))

$$\tilde{\mathbf{d}}^{(k)} := t \nabla f(\tilde{\mathbf{x}}^{(k)}) + t \boldsymbol{\sigma}_1^{(k)} + \boldsymbol{\sigma}_2^{(k)},$$

where $\boldsymbol{\sigma}_1^{(k)}, \boldsymbol{\sigma}_2^{(k)}$ depend on the two rounding schemes used for the evaluation of the gradient and the multiplication by t . In particular, we have:

$$\tilde{\mathbf{x}}^{(k+1)} = \tilde{\mathbf{x}}^{(k)} - \tilde{\mathbf{d}}^{(k)}. \quad (13)$$

From (10), we have that $\|\boldsymbol{\sigma}_1^{(k)}\|_\infty \leq mu$, where m is a positive constant depending on the gradient function and $\tilde{\mathbf{x}}$; $\|\boldsymbol{\sigma}_2^{(k)}\|_\infty \leq \frac{1}{2}u$ and $\|\boldsymbol{\sigma}_2^{(k)}\|_\infty < u$ for RN and stochastic rounding, respectively. In particular, both signs of the elements and magnitude of $\tilde{\mathbf{d}}^{(k)}$ are crucial to understanding the convergence of GD. In the next subsection, we distinguish three cases that describe the number of components of the updating vector that have magnitudes close to the rounding errors. We explore the roles of $\boldsymbol{\sigma}_1^{(k)}$ and $\boldsymbol{\sigma}_2^{(k)}$ in determining properties of $\tilde{\mathbf{d}}^{(k)}$. We start by studying a condition that ensures that $\tilde{\mathbf{d}}^{(k)}$ has a non-descent direction.

3.1 A condition for the non-opposite sign property

Intuitively, it is desirable to have that the entries of $\tilde{\mathbf{d}}^{(k)}$ have non-opposite signs to the corresponding entries of $\nabla f(\tilde{\mathbf{x}}^{(k)})$, as this property implies that $\mathbf{x}^{(k+1)}$ updates in a non-ascent direction. Taking a closer look at (5) we see that $\boldsymbol{\sigma}_2^{(k)}$, resulting from a multiplication, can not result in an opposite sign. On the other hand, in view of (10), $\boldsymbol{\sigma}_1^{(k)}$ plays a significant role when some of the entries of the exact gradient verify $|\nabla f(\tilde{\mathbf{x}}^{(k)})_i| < |\sigma_{1,i}^{(k)}|$. In this case, GD may still update in a descent direction, i.e., $\nabla f(\tilde{\mathbf{x}}^{(k)})^T \tilde{\mathbf{d}}^{(k)} > 0$; however, we cannot guarantee the monotonicity of the objective function values in general and, often, zigzag behavior is observed in the neighborhood of the optimal points. The influence of errors in evaluating the gradient function on the convergence of stochastic or inexact gradient descent has been extensively analyzed in many studies [26–28]. It has been shown that even using exact arithmetic for the other computations, the linear or sublinear convergence rate can be proven only up to a neighborhood of a stationary point, where the majority of the gradient components are small [28].

In our study, we focus on the utilization of rounding methods to implement GD in finite-precision arithmetic, with an additional assumption ensuring that the evaluation of the gradient does not introduce a change in sign with respect to the exact quantity. That is, for convenience our analysis assumes that for all iterations we have

$$|\nabla f(\tilde{\mathbf{x}}^{(k)})_i| \geq |\sigma_{1,i}^{(k)}|, \quad i = 1, \dots, n. \quad (14)$$

In this situation, GD is ensured to update in a non-ascent direction as (14) implies that

$$\text{sign}(t \nabla f(\tilde{\mathbf{x}}^{(k)})_i) \text{sign}(t \nabla f(\tilde{\mathbf{x}}^{(k)})_i + t \sigma_{1,i}^{(k)} + \sigma_{2,i}^{(k)}) \geq 0 \quad i = 1, \dots, n.$$

Note that condition (14) is a very reasonable assumption, as it indicates that the rounding error in evaluating the components of the gradient is not larger than the true quantities. We remark that assumption (14) may be relaxed, by only requiring that in every iteration there is at least one component i satisfying $|\nabla f(\tilde{\mathbf{x}}^{(k)})_i| > |\sigma_{1,i}^{(k)}|$, if we slightly update the GD procedure. Namely, when we set all components of $\tilde{\mathbf{d}}^{(k)}$ that do not satisfy (14) to zero, then the modified direction vector is still a descent direction. We do not analyze this modified GD procedure because, in practice, it might be too conservative to stop updating coordinates as soon as they violate (14); in addition, the theoretical analysis appears more technical, although it follows similar arguments.

Together with the Lipschitz continuity property (1), (14) implies the lower bound $\|\tilde{\mathbf{x}}^{(k)} - \mathbf{x}^*\| \geq L^{-1} \|\boldsymbol{\sigma}_1^{(k)}\|$, which means that in the context of low precision, GD may not converge arbitrarily close to the optimal point. In subsection 6.3, we show an example (cf. Figure 7) where GD converges to the exact optimal point when it is representable in finite precision and otherwise converges to a neighborhood of the optimal point whose size depends on u .

3.2 Recap of the general assumptions

So far, we have discussed several reasonable assumptions concerning the objective function, the number format, and the rounding operation. To get concise statements in our convergence analysis and to make it easier for the reader to retrieve these properties, in the following, we recap the conditions assumed for all the theoretical statements in this paper.

Assumption 1.

1. The objective function f satisfies (1) and (2) with constant $0 < \mu \leq \frac{1}{2}L$.
2. The evaluation of the components of ∇f satisfies the assumption of Proposition 2. Moreover, the parameter c is bounded above by a polynomial function of L, χ , and n .
3. For every iteration step, the absolute error $\boldsymbol{\sigma}_1^{(k)}$ caused by evaluating the gradient satisfies (14).
4. The quantities $\mathbf{x}^{(0)}$ and t are exactly represented in the chosen number format.
5. All the iterates of GD are in a compact space such that $\|\tilde{\mathbf{x}}^{(k)} - \mathbf{x}^*\| \leq \chi$ for all k .
6. Overflow is not encountered during computations.

Note that the conditions 1 and 5 in Assumption 1 imply that $\|\nabla f(\tilde{\mathbf{x}}^{(k)})\| \leq L\chi$. Overflow is not considered in this study, because the primary focus of this paper is on addressing the stagnation problem of GD, which is often caused by limited precision of fractional bits. In the recent study of NVIDIA [29], it addresses the importance of preventing gradients from being rounded to zero in the 16-bit representation and it

also indicates that even if an overflow occurs, infrequent skipping of weight updates results in the same training accuracy as that of 32-bit training.

3.3 The magnitude of the updating vector

Together with the non-opposite sign property discussed in the previous subsection, the magnitude of the entries in $\tilde{\mathbf{d}}^{(k)}$ plays a crucial role in analyzing the convergence properties of GD. However, it is reasonable to observe varying magnitudes among the different components of the gradient during the execution of GD. For this reason, we identify and subdivide our theoretical analysis for the following three cases.

Condition of Case I. $|\nabla f(\tilde{\mathbf{x}}^{(k)})_i + \sigma_{1,i}^{(k)}| \geq \frac{u}{t}, \quad i = 1, \dots, n. \quad (15)$

Condition of Case II. $|\nabla f(\tilde{\mathbf{x}}^{(k)})_i + \sigma_{1,i}^{(k)}| < \frac{u}{t}, \quad i = 1, \dots, n. \quad (16)$

Condition of Case III. There exist disjoint non-empty subsets of indices $\mathcal{C}_1, \mathcal{C}_2$ such that $\mathcal{C}_1 \cup \mathcal{C}_2 = \{1, \dots, n\}$ and

$$|\nabla f(\tilde{\mathbf{x}}^{(k)})_i + \sigma_{1,i}^{(k)}| \geq \frac{u}{t}, \quad \text{for } i \in \mathcal{C}_1, \quad |\nabla f(\tilde{\mathbf{x}}^{(k)})_i + \sigma_{1,i}^{(k)}| < \frac{u}{t}, \quad \text{for } i \in \mathcal{C}_2. \quad (17)$$

As discussed, Case I mostly characterizes the early stages of the updating procedure of GD. Conversely, Cases II and III come into play when, at a later stage of the process, some or all the rounded gradient components approach the rounding precision threshold u . For a practical demonstration, in subsection 6.3 we demonstrate the occurrence of these three cases in the GD updating process in the context of Himmelblau’s function; see, e.g., Figure 7d. Considering the general expression for GD’s iteration (13), we can reformulate $\tilde{\mathbf{d}}^{(k)}$ for these three conditions.

Case I. In this case the magnitude of the i th component of $\tilde{\mathbf{d}}^{(k)}$ (cf. (15)) mainly depends on $\nabla f(\tilde{\mathbf{x}}^{(k)})_i$ and we informally say that *the updating procedure of GD is dominated by the gradient*. Let us rewrite the updating vector as

$$\tilde{\mathbf{d}}^{(k)} = t \nabla f(\tilde{\mathbf{x}}^{(k)}) \circ (\mathbf{1} + \mathbf{r}^{(k)}), \quad (18)$$

where \circ is the Hadamard (component-wise) product and $\mathbf{r}^{(k)}$ is a vector of the relative errors with respect to the exact quantity $t \nabla f(\tilde{\mathbf{x}}^{(k)})$, whose entries are given by

$$r_i^{(k)} = \frac{t \sigma_{1,i}^{(k)} + \sigma_{2,i}^{(k)}}{t \nabla f(\tilde{\mathbf{x}}^{(k)})_i}, \quad \text{for } i = 1, \dots, n. \quad (19)$$

Equations (14) and (15) imply bounds on the entries of $\mathbf{r}^{(k)}$; indeed, we have the following result and the proof is available in Appendix A.

Lemma 3. *Under the Assumption 1 (cf. (14)) and the condition of Case I (15), for $i = 1, \dots, n$, we have that $-1 < r_i^{(k)} < 3$.*

Case II. Condition (16) shows that $\sigma_2^{(k)}$ has a crucial impact on determining the magnitude of $\tilde{\mathbf{d}}^{(k)}$. All the entries of the updating vector belong to the set $\{0, u, -u\}$ and, if RN is employed, it is likely that GD stagnates. In this case, *the updating procedure of GD is dominated by the rounding errors*. The updating vector is generated according to the rule

$$\tilde{d}_i^{(k)} = \begin{cases} 0, & \text{with probability } p(t \nabla f(\mathbf{x}^{(k)})_i + t \sigma_{1,i}^{(k)}), \\ \text{sign}(\nabla f(\mathbf{x}^{(k)})_i + \sigma_{1,i}^{(k)}) u, & \text{with probability } 1 - p(t \nabla f(\mathbf{x}^{(k)})_i + t \sigma_{1,i}^{(k)}). \end{cases} \quad (20)$$

Here, $p \in \{p_r, p_0, p_\varepsilon, p_{\varepsilon s}\}$ depends on the rounding method employed, which is introduced in subsection 2.2. This updating rule is similar to the approach of the *sign gradient descent method* by [30], except for the stochastic dependence of our scheme.

Case III. The last case refers to situations where the components of the gradient vector have different scales. In this case, we may encounter entries on the level of rounding errors while others are close to the value of the exact partial derivatives. We informally say that *the updating procedure of GD is partially dominated by the gradient and partially dominated by the rounding errors*. More explicitly, in Case III the updating vector is generated as follows:

$$\begin{aligned} i \in \mathcal{C}_1 &\Rightarrow \tilde{d}_i^{(k)} = t \nabla f(\tilde{\mathbf{x}}^{(k)})_i (1 + r_i^{(k)}); \\ i \in \mathcal{C}_2 &\Rightarrow \tilde{d}_i^{(k)} = \begin{cases} 0, & \text{with probability } p(t \nabla f(\mathbf{x}^{(k)})_i + t \sigma_{1,i}^{(k)}), \\ \text{sign}(\nabla f(\mathbf{x}^{(k)})_i + \sigma_{1,i}^{(k)}) u, & \text{with probability } 1 - p(t \nabla f(\mathbf{x}^{(k)})_i + t \sigma_{1,i}^{(k)}), \end{cases} \end{aligned} \quad (21)$$

which may be viewed as a combination of (18) and (20).

In the next section, we provide an analysis of the convergence of GD for all three cases, regarding two aspects: the monotonicity and the convergence rate.

4 Convergence analysis of GD with fixed-point arithmetic

Under Assumption 1, when using stochastic rounding, the quantities $\tilde{\mathbf{d}}^{(k)}$, $\tilde{\mathbf{x}}^{(k)}$, and $\nabla f(\tilde{\mathbf{x}}^{(k)})$ can be viewed as random vectors obtained by GD. We prove that for the objective functions satisfying Assumption 1, the linear convergence of GD in exact arithmetic (cf. Theorem 1) can be extended to our framework (5). We begin by analyzing the updating direction of rounding errors for different stochastic rounding methods.

4.1 The direction of stochastic rounding errors

Taking the expectation of $\nabla f(\tilde{\mathbf{x}}^{(k)})^T \tilde{\mathbf{d}}^{(k)}$ in (13), we have

$$\begin{aligned} \mathbb{E}[\nabla f(\tilde{\mathbf{x}}^{(k)})^T \tilde{\mathbf{d}}^{(k)}] &= \mathbb{E}[\nabla f(\tilde{\mathbf{x}}^{(k)})^T (t \nabla f(\tilde{\mathbf{x}}^{(k)}) + t \sigma_1^{(k)} + \sigma_2^{(k)})] \\ &= t \mathbb{E}[\|\nabla f(\tilde{\mathbf{x}}^{(k)})\|^2] + t \mathbb{E}[\nabla f(\tilde{\mathbf{x}}^{(k)})^T \sigma_1^{(k)}] + \mathbb{E}[\nabla f(\tilde{\mathbf{x}}^{(k)})^T \sigma_2^{(k)}]. \end{aligned}$$

We see that both $\sigma_1^{(k)}$ and $\sigma_2^{(k)}$ may result in a different updating direction and distance from the exact updating procedure. One may choose the stepsize t to influence the term $E[\nabla f(\tilde{\mathbf{x}}^{(k)})^T \sigma_1^{(k)}]$; however, the choice of t only affects the probability of rounding up or down for $\nabla f(\tilde{\mathbf{x}}^{(k)})^T \sigma_2^{(k)}$, so that the influence on $E[\nabla f(\tilde{\mathbf{x}}^{(k)})^T \sigma_2^{(k)}]$ may be mild.

Now, we study the quantity $E[\nabla f(\tilde{\mathbf{x}}^{(k)})^T \sigma_1^{(k)}]$ for different stochastic rounding methods. We have the following result; for the proof see Appendix A.

Lemma 4. *Under Assumption 1, if SR is applied for evaluating σ_1 , then it holds*

$$E[\nabla f(\tilde{\mathbf{x}}^{(k)})^T (\nabla f(\tilde{\mathbf{x}}^{(k)}) + \sigma_1^{(k)})] \simeq E[\|\nabla f(\tilde{\mathbf{x}}^{(k)})\|^2],$$

where \simeq is defined in section 1.

The proof of Lemma 4 shows that when $L\chi\sqrt{n}u^2$ is negligible, SR causes the expectation of the inner product $\nabla f(\tilde{\mathbf{x}}^{(k)})^T \text{SR}(\nabla f(\tilde{\mathbf{x}}^{(k)}))$ to coincide with the corresponding quantity in exact arithmetic, i.e.,

$$E[\nabla f(\tilde{\mathbf{x}}^{(k)})^T \text{SR}(\nabla f(\tilde{\mathbf{x}}^{(k)}))] \simeq E[\|\nabla f(\tilde{\mathbf{x}}^{(k)})\|^2].$$

Unfortunately, this is not the case for SR_ε because it is hard to determine $E[\sigma_1]$ when the value of $E[\nabla f(\tilde{\mathbf{x}}^{(k)})]$ is unknown. To circumvent this problem-dependent behavior of SR_ε , we only consider the use of SR to evaluate all the gradients in our analysis.

Now, let us study the quantity $E[\nabla f(\tilde{\mathbf{x}}^{(k)})^T \sigma_2^{(k)}]$ under the use of SR and its zero bias property.

Lemma 5. *If σ_2 is obtained using SR, then it holds $E[\nabla f(\tilde{\mathbf{x}}^{(k)})^T \sigma_2^{(k)}] = 0$.*

We omit the proof of Lemma 5, since it can be simply derived from $E[\sigma_{2,i}^{(k)} | \nabla f(\tilde{\mathbf{x}}^{(k)})_i, \sigma_{1,i}^{(k)}] = 0$ for all i and utilizing the law of total expectation (e.g., [31, (1.14)]). On the other hand, if we apply SR_ε we obtain, on average, an additional contribution in an ascent direction.

Lemma 6. *If σ_2 is the result of SR_ε , $\nabla f(\tilde{\mathbf{x}}^{(k)})$ is not identically zero, and (14) is satisfied, then $E[\nabla f(\tilde{\mathbf{x}}^{(k)})^T \sigma_2^{(k)}] > 0$.*

The proof is available in Appendix A. In the next section, we will use the results stated here as building blocks for studying the impact of rounding errors on the convergence of GD.

4.2 Convergence analysis of GD for the three cases

Let us proceed to analyze the convergence of GD in the three cases introduced in subsection 3.3. For each case, we provide conditions to ensure that the sequence generated by GD has decreasing objective function values. Moreover, we quantify the rate of convergence based on the number of steps that GD spends in each case.

4.2.1 Case I

We start by observing that the condition of Case I (15) implies $2t |\nabla f(\tilde{\mathbf{x}}^{(k)})_i| \geq u$, $i = 1, \dots, n$, which leads to

$$\|\nabla f(\tilde{\mathbf{x}}^{(k)})\| \geq \frac{1}{2} \sqrt{n} \frac{u}{t}. \quad (22)$$

In view of (1), (22) implies $\|\mathbf{x}^{(k)} - \mathbf{x}^*\| \geq \frac{1}{2} L^{-1} \sqrt{n} \frac{u}{t}$, where $\mathbf{x}^* \in \mathcal{X}^*$. Together with the inequality (22), it tells us that GD can satisfy the condition of Case I only outside a neighborhood of \mathcal{X}^* .

We commence the study of the objective function values associated with the sequence generated by GD in finite precision. Let us denote the minimum ratio between the exact entries and the rounded entries of $t \nabla f(\tilde{\mathbf{x}}^{(j)})$ at the j th iterate by

$$\gamma_j := \min_{i=1, \dots, n} 1 + r_i^{(j)},$$

so that $\gamma_j \in (0, 4)$ (see Lemma 3). Adapting the proof of [10, Theorem 1] to our framework, we obtain the following result for general rounding errors.

Theorem 7. *Under Assumption 1, consider k iteration steps of GD in fixed-point arithmetic with a fixed stepsize $t \leq \frac{1}{4L}$. Suppose that the condition of Case I (15) is satisfied throughout these k iteration steps. Then, the k th iterate satisfies*

$$f(\tilde{\mathbf{x}}^{(k)}) - f^* \leq \prod_{j=0}^{k-1} (1 - t \mu \gamma_j) (f(\mathbf{x}^{(0)}) - f^*), \quad (23)$$

where $0 < t \mu \gamma_j < \frac{1}{2}$, $j = 0, \dots, k-1$.

Proof. The Lipschitz gradient property (cf. (1)) and (18) allow us to write

$$\begin{aligned} f(\tilde{\mathbf{x}}^{(k+1)}) &\leq f(\tilde{\mathbf{x}}^{(k)}) - \nabla f(\tilde{\mathbf{x}}^{(k)})^T \tilde{\mathbf{d}}^{(k)} + \frac{1}{2} L \|\tilde{\mathbf{d}}^{(k)}\|^2 \\ &= f(\tilde{\mathbf{x}}^{(k)}) - t \sum_{i=1}^n (1 + r_i^{(k)}) (1 - \frac{1}{2} L t (1 + r_i^{(k)})) (\nabla f(\tilde{\mathbf{x}}^{(k)})_i)^2. \end{aligned}$$

Since $t \leq \frac{1}{4L}$ and $0 < 1 + r_i^{(k)} < 4$ (Lemma 3), we have that

$$f(\tilde{\mathbf{x}}^{(k+1)}) \leq f(\tilde{\mathbf{x}}^{(k)}) - \frac{1}{2} t \sum_{i=1}^n (1 + r_i^{(k)}) (\nabla f(\tilde{\mathbf{x}}^{(k)})_i)^2, \quad (24)$$

which in turn implies

$$\begin{aligned} f(\tilde{\mathbf{x}}^{(k+1)}) - f^* &\leq f(\tilde{\mathbf{x}}^{(k)}) - f^* - \frac{1}{2} t \gamma_k \|\nabla f(\tilde{\mathbf{x}}^{(k)})\|^2 \\ &\stackrel{(2)}{\leq} f(\tilde{\mathbf{x}}^{(k)}) - f^* - t \mu \gamma_k (f(\tilde{\mathbf{x}}^{(k)}) - f^*) \end{aligned}$$

$$= (1 - t\mu\gamma_k)(f(\tilde{\mathbf{x}}^{(k)}) - f^*). \quad (25)$$

The assumptions $\mu \leq \frac{1}{2}L$, $t \leq \frac{1}{4L}$, and $\gamma_k < 4$, yield $1 - t\mu\gamma_k \in (\frac{1}{2}, 1)$. By expanding the recursive definition of (25), we obtain the required result. \square

Comparing Theorems 1 and 7, in the presence of rounding errors, a smaller t is required to ensure the monotonicity of GD. In particular, the bound on t depends on the upper bound on the relative rounding errors of $t \nabla f(\tilde{\mathbf{x}}^{(k)})$. In other words, a larger $r_i^{(k)}$ in (19) leads to a smaller bound on t . Moreover, when rounding errors are zeros, i.e., $\gamma_j = 1$ in (23) for all j , Theorem 7 yields the same bound on the convergence rate achieved by exact arithmetic (cf. (4)). When $\gamma_j < 1$, the rounding errors may result in slower convergence of GD compared to that in Theorem 1. Furthermore, on the basis of (24), we see that stagnation may occur only if $r_i^{(j)} = -1$ for all i . Since $r_i^{(j)} > -1$ under Assumption 1 and (15) (cf. Lemma 3), we have that in Case I, GD does not suffer from stagnation.

Interestingly, Theorem 7 also states that a faster convergence rate may be achieved when many of the γ_j s are larger than 1 (again, comparing with (4)). Next, we show that we may achieve this, on average, when σ_2 is the result of SR_ε . Before presenting the result, we introduce and comment on a quantity that is important for our analysis:

$$\rho_k := \min_{i=1, \dots, n} \frac{n \mathbb{E}[\sigma_{2,i}^{(k)} \nabla f(\tilde{\mathbf{x}}^{(k)})_i]}{\mathbb{E}[\|\nabla f(\tilde{\mathbf{x}}^{(k)})\|^2]}. \quad (26)$$

The value of ρ_k measures the minimum ratio between the expected rounding errors and the expected squared norm of the gradient at the k th iteration. According to Lemmas 4 and 5, it is easy to check that when σ_2 is obtained by the use of SR, we have $\rho_j = 0$ for $j = 1, \dots, k$. When SR_ε is applied, we can instead rely on the following upper bound.

Lemma 8. *If σ_2 is obtained using SR_ε , under the condition of Case I (15), we have the inequality $0 < \rho_k \leq 2t\varepsilon$.*

The proof of Lemma 8 is available in the Appendix A. We are now ready to analyze the convergence rate for SR_ε . To facilitate the analysis, let us denote the minimum value of ρ_j over the iteration steps as

$$\tau_1 := \min_{j=0, \dots, k-1} \rho_j. \quad (27)$$

Based on Lemma 8, we have $\tau_1 \in (0, 2t\varepsilon]$.

Theorem 9. *Under Assumption 1, after k iteration steps of GD in fixed-precision arithmetic with a fixed stepsize t such that $t \leq \frac{1}{4L}$ and suppose that the condition of Case I (15) is satisfied throughout the k iteration steps. If σ_1 and σ_2 in (5) are obtained using SR and SR_ε , respectively, then with τ_1 as in (27), we have*

$$\mathbb{E}[f(\tilde{\mathbf{x}}^{(k)}) - f^*] \lesssim (1 - \mu(t + \tau_1))^k (f(\mathbf{x}^{(0)}) - f^*), \quad (28)$$

$\tau_1 \in (0, 2t\varepsilon]$ and $\mu(t + \tau_1) < 1$, where \lesssim is the notation described in section 1.

Proof. Substituting (19) into (24), and taking the expectation of both sides, we obtain

$$\begin{aligned} \mathbb{E}[f(\tilde{\mathbf{x}}^{(k+1)}) - f^*] &\leq \mathbb{E}[f(\tilde{\mathbf{x}}^{(k)}) - f^*] - \frac{1}{2}t \mathbb{E}[\|\nabla f(\tilde{\mathbf{x}}^{(k)})\|^2] \\ &\quad - \frac{1}{2} \sum_{i=1}^n (t \mathbb{E}[\sigma_{1,i}^{(k)} \nabla f(\tilde{\mathbf{x}}^{(k)})_i] + \mathbb{E}[\sigma_{2,i}^{(k)} \nabla f(\tilde{\mathbf{x}}^{(k)})_i]). \end{aligned} \quad (29)$$

In view of Lemmas 4 and 6, we have $\mathbb{E}[\|\nabla f(\tilde{\mathbf{x}}^{(k)})\|^2] + \mathbb{E}[\sigma_{1,i}^{(k)} \nabla f(\tilde{\mathbf{x}}^{(k)})_i] \simeq \mathbb{E}[\|\nabla f(\tilde{\mathbf{x}}^{(k)})\|^2]$ and $\mathbb{E}[\sigma_{2,i}^{(k)} \nabla f(\tilde{\mathbf{x}}^{(k)})_i] > 0$. Furthermore, (26) and (29) imply that

$$\mathbb{E}[f(\tilde{\mathbf{x}}^{(k+1)}) - f^*] \lesssim \mathbb{E}[f(\tilde{\mathbf{x}}^{(k)}) - f^*] - \frac{1}{2}t \mathbb{E}[\|\nabla f(\tilde{\mathbf{x}}^{(k)})\|^2] - \frac{1}{2}\rho_k \mathbb{E}[\|\nabla f(\tilde{\mathbf{x}}^{(k)})\|^2]. \quad (30)$$

Taking the expectation of (2), we obtain

$$\mathbb{E}[\|\nabla f(\tilde{\mathbf{x}}^{(k)})\|^2] \geq 2\mu \mathbb{E}[f(\tilde{\mathbf{x}}^{(k)}) - f^*]. \quad (31)$$

Hence, substituting (31) into (30), we have

$$\mathbb{E}[f(\tilde{\mathbf{x}}^{(k+1)}) - f^*] \lesssim (1 - (t + \rho_k)\mu) \mathbb{E}[f(\tilde{\mathbf{x}}^{(k)}) - f^*].$$

Expanding the recursion, we obtain

$$\mathbb{E}[f(\tilde{\mathbf{x}}^{(k)}) - f^*] \lesssim \prod_{j=0}^{k-1} (1 - (t + \rho_j)\mu) \mathbb{E}[f(\mathbf{x}^{(0)}) - f^*].$$

According to Lemma 8, we have the claim for $\tau_1 \in (0, 2t\varepsilon]$. Furthermore, the properties $\varepsilon < 1$, $\rho_j \leq 2t\varepsilon$ and $\mu \leq L/2$ yield $(t + \rho_j)\mu \leq \frac{1+2\varepsilon}{8} < \frac{3}{8}$. \square

Looking at (26), a larger value of ε in SR_ε might allow a larger bound for τ_1 . Comparing Theorem 1 (cf. (4)) and Theorem 9 (cf. (28)), when choosing the same t , we have that a tighter bound on convergence rate, in expectation, is obtained by using SR_ε .

When both σ_1 and σ_2 are obtained by SR, Lemma 5 implies $\mathbb{E}[\sigma_{2,i}^{(k)} \nabla f(\tilde{\mathbf{x}}^{(k)})_i] = 0$, which yields $\rho_k = 0$ in (29). Together with Lemma 4, this gives, in expectation, the same convergence rate that holds for infinite-precision computations.

Corollary 10. *Under the same assumptions of Theorem 9, if σ_2 is obtained using SR, then we have*

$$\mathbb{E}[f(\tilde{\mathbf{x}}^{(k)}) - f^*] \lesssim (1 - t\mu)^k (f(\mathbf{x}^{(0)}) - f^*).$$

We omit the proof of Corollary 10 since it can be easily obtained on the basis of Lemma 5 and by proceeding analogously to the proof of Theorem 9. Both Theorem 9 and Corollary 10 indicate that smaller values of t are required to ensure the convergence of GD compared to the case of the exact computation. This is because their

analysis relies on the worst-case bound of σ_1 . In the simulation studies reported in section 6, we will demonstrate that these restrictions are usually pessimistic and, in practice, t can be chosen as large as the upper bound in Theorem 1, that is $t \leq \frac{1}{L}$.

4.2.2 Case II

In Case II, each of the entries of the updating vector $\tilde{\mathbf{d}}^{(k)}$ takes one of the values in $\{0, u, -u\}$; when it is 0, property (14) implies that $\nabla f(\tilde{\mathbf{x}}^{(k)})_i = 0$. Therefore, we have $\sigma_{2,i} = 0$, which does not influence the convergence of GD. For our analysis, it is convenient to single out the cases where the rounded gradient has some components that are exactly zero. More formally, we denote the finite set of nonzero values that the i th component of $\nabla f(\tilde{\mathbf{x}}^{(k)})$ may assume by $\mathcal{W}_i^{(k)}$. Note that $\mathcal{W}_i^{(k)}$ can be empty for some entries of $\nabla f(\tilde{\mathbf{x}}^{(k)})$, but when it is empty for all i , in accordance with (14), it implies that $\nabla f(\tilde{\mathbf{x}}^{(k)}) = 0$ and GD has reached a stationary point. Additionally, (20) shows that GD is highly likely to reach a state of stagnation when the quantity $t \nabla f(\mathbf{x}^{(k)})_i + t \sigma_{1,i}^{(k)}$ is small. In particular, when $t \nabla f(\mathbf{x}^{(k)})_i + t \sigma_{1,i}^{(k)} < \frac{u}{2}$, the use of RN will cause $\tilde{d}_i^{(k)} = 0$, resulting in the stagnation of GD. In the following propositions, we show that the use of stochastic rounding can ensure the monotonicity of the objective function and achieve linear convergence of GD. Before we start our analysis, we recall a basic property of conditional expectation to facilitate further proof.

For random variables X, Y, Z we have (see, e.g., [32, (10.40)])

$$\mathbb{E}[\mathbb{E}[X \mid Y, Z] \mid Y] = \mathbb{E}[X \mid Y]. \quad (32)$$

When stochastic rounding is employed, our aim is to prove that GD achieves a linear convergence rate until it reaches a neighborhood around \mathbf{x}^* . To shed light on the size of this neighborhood, we introduce the quantity

$$\theta_k := \min_{i=1, \dots, n} \min_{\nabla f(\tilde{\mathbf{x}}^{(k)})_i \in \mathcal{W}_i^{(k)}} \frac{2 |\nabla f(\tilde{\mathbf{x}}^{(k)})_i| - Lu}{|\nabla f(\tilde{\mathbf{x}}^{(k)})_i|}, \quad (33)$$

which implies that $\theta_k < 2$. The value of θ_k is approximately equal to 2 when the gradient's components are large compared to Lu , which is typically the case at the beginning of the process. Only when at least one entry of the gradient gets close to 0, θ_k may be no longer positive. In this case, where some of the gradient components are near zero, rounding errors can play a positive or negative role in determining whether GD converges, stagnates, or oscillates. When these rounding errors are intentionally designed to align in a descent direction, such as when using SR_ε , then it may help the optimization process; see for instance Figure 3b.

In the subsequent convergence analysis, we show that the condition $\theta_k > 0$ provides, in expectation, strict monotonicity and linear convergence rate. Note that $\theta_k > 0$ implies that $|\nabla f(\tilde{\mathbf{x}}^{(k)})_i| > \frac{1}{2} Lu$. This observation does not contradict condition (16). This is due to the fact that (16) provides an upper bound on the rounded gradient, which means that even if $|\nabla f(\tilde{\mathbf{x}}^{(k)})_i|$ is larger than $\frac{1}{2} Lu$, the rounded gradient can still be small, possibly even reaching 0. We begin with the monotonicity when using SR.

Proposition 11. *Under Assumption 1, after k iteration steps of GD in fixed-precision arithmetic with a fixed stepsize $t \leq \frac{1}{L}$, suppose that the condition of Case II (16) has been satisfied throughout the k iteration steps. If σ_1 and σ_2 in (5) are obtained by SR and $\theta_k > 0$ in (33) then*

$$\mathbb{E}[f(\tilde{\mathbf{x}}^{(k)})] < \mathbb{E}[f(\tilde{\mathbf{x}}^{(k-1)})].$$

Proof. The Lipschitz gradient property (1), rephrased in terms of expectations, yields

$$\mathbb{E}[f(\tilde{\mathbf{x}}^{(k+1)})] \leq \mathbb{E}[f(\tilde{\mathbf{x}}^{(k)})] - \sum_{i=1}^n \mathbb{E}[\nabla f(\tilde{\mathbf{x}}^{(k)})_i \tilde{d}_i^{(k)} - \frac{1}{2} L (\tilde{d}_i^{(k)})^2]. \quad (34)$$

According to (32), we have

$$\mathbb{E}[\nabla f(\tilde{\mathbf{x}}^{(k)})_i \sigma_{2,i}^{(k)} \mid \nabla f(\tilde{\mathbf{x}}^{(k)})_i] = \mathbb{E}[\mathbb{E}[\nabla f(\tilde{\mathbf{x}}^{(k)})_i \sigma_{2,i}^{(k)} \mid \nabla f(\tilde{\mathbf{x}}^{(k)})_i, \sigma_{1,i}^{(k)}] \mid \nabla f(\tilde{\mathbf{x}}^{(k)})_i] = 0.$$

Therefore, letting q vary over $\mathcal{W}_i^{(k)}$, the set of all the possible values of $\nabla f(\tilde{\mathbf{x}}^{(k)})_i$, and utilizing the law of total expectation, we have

$$\begin{aligned} & \mathbb{E}[\nabla f(\tilde{\mathbf{x}}^{(k)})_i \tilde{d}_i^{(k)}] \\ &= \sum_{q \in \mathcal{W}_i^{(k)}} \mathbb{E}[\nabla f(\tilde{\mathbf{x}}^{(k)})_i \tilde{d}_i^{(k)} \mid \nabla f(\tilde{\mathbf{x}}^{(k)})_i = q] P(\nabla f(\tilde{\mathbf{x}}^{(k)})_i = q) \\ &= \sum_{q \in \mathcal{W}_i^{(k)}} \mathbb{E}[\nabla f(\tilde{\mathbf{x}}^{(k)})_i (t \nabla f(\tilde{\mathbf{x}}^{(k)})_i + t \sigma_{1,i}^{(k)}) \mid \nabla f(\tilde{\mathbf{x}}^{(k)})_i = q] P(\nabla f(\tilde{\mathbf{x}}^{(k)})_i = q). \end{aligned} \quad (35)$$

Similarly, we have

$$\mathbb{E}[(\tilde{d}_i^{(k)})^2] = \sum_{q \in \mathcal{W}_i^{(k)}} \mathbb{E}[(\tilde{d}_i^{(k)})^2 \mid \nabla f(\tilde{\mathbf{x}}^{(k)})_i = q] P(\nabla f(\tilde{\mathbf{x}}^{(k)})_i = q).$$

Based on (20), when $\nabla f(\tilde{\mathbf{x}}^{(k)})_i + \sigma_{1,i}^{(k)} > 0$, we have

$$(\tilde{d}_i^{(k)})^2 = \text{SR}(t \nabla f(\tilde{\mathbf{x}}^{(k)})_i + t \sigma_{1,i}^{(k)})^2 = \begin{cases} 0, & \text{with probability } p_0(t \nabla f(\tilde{\mathbf{x}}^{(k)})_i + t \sigma_{1,i}^{(k)}), \\ u^2, & \text{with probability } 1 - p_0(t \nabla f(\tilde{\mathbf{x}}^{(k)})_i + t \sigma_{1,i}^{(k)}). \end{cases}$$

Replacing x by $t \nabla f(\tilde{\mathbf{x}}^{(k)})_i + t \sigma_{1,i}^{(k)}$ in (7), we have

$$\mathbb{E}[\tilde{d}_i^{(k)} \mid \nabla f(\tilde{\mathbf{x}}^{(k)})_i, \sigma_{1,i}^{(k)}] = t \nabla f(\tilde{\mathbf{x}}^{(k)})_i + t \sigma_{1,i}^{(k)} = u(1 - p_0(t \nabla f(\tilde{\mathbf{x}}^{(k)})_i + t \sigma_{1,i}^{(k)})),$$

so that

$$\mathbb{E}[(\tilde{d}_i^{(k)})^2 \mid \nabla f(\tilde{\mathbf{x}}^{(k)})_i, \sigma_{1,i}^{(k)}] = u^2(1 - p_0(t \nabla f(\tilde{\mathbf{x}}^{(k)})_i + t \sigma_{1,i}^{(k)})) = u |t \nabla f(\tilde{\mathbf{x}}^{(k)})_i + t \sigma_{1,i}^{(k)}|. \quad (36)$$

It is easy to check that (36) also holds for the condition when $\nabla f(\tilde{\mathbf{x}}^{(k)})_i + \sigma_{1,i}^{(k)} < 0$. In view of (32), we have

$$\mathbb{E}[(\tilde{d}_i^{(k)})^2 \mid \nabla f(\tilde{\mathbf{x}}^{(k)})_i] = \mathbb{E}[\mathbb{E}[(\tilde{d}_i^{(k)})^2 \mid \nabla f(\tilde{\mathbf{x}}^{(k)})_i, \sigma_{1,i}^{(k)}] \mid \nabla f(\tilde{\mathbf{x}}^{(k)})_i],$$

which leads to

$$\mathbb{E}[(\tilde{d}_i^{(k)})^2] = \sum_{q \in \mathcal{W}_i^{(k)}} \mathbb{E}[|t \nabla f(\tilde{\mathbf{x}}^{(k)})_i + t \sigma_{1,i}^{(k)}| u \mid \nabla f(\tilde{\mathbf{x}}^{(k)})_i = q] P(\nabla f(\tilde{\mathbf{x}}^{(k)})_i = q).$$

Equation (14) implies that

$$\nabla f(\tilde{\mathbf{x}}^{(k)})_i (t \nabla f(\tilde{\mathbf{x}}^{(k)})_i + t \sigma_{1,i}^{(k)}) = |\nabla f(\tilde{\mathbf{x}}^{(k)})_i| |t \nabla f(\tilde{\mathbf{x}}^{(k)})_i + t \sigma_{1,i}^{(k)}|,$$

and together with (35), it yields

$$\begin{aligned} & \mathbb{E}[\nabla f(\tilde{\mathbf{x}}^{(k)})_i \tilde{d}_i^{(k)} - \frac{1}{2} L (\tilde{d}_i^{(k)})^2] \\ &= \sum_{q \in \mathcal{W}_i^{(k)}} \mathbb{E}[|t \nabla f(\tilde{\mathbf{x}}^{(k)})_i + t \sigma_{1,i}^{(k)}| (|\nabla f(\tilde{\mathbf{x}}^{(k)})_i| - \frac{1}{2} L u) \mid \nabla f(\tilde{\mathbf{x}}^{(k)})_i = q] P(\nabla f(\tilde{\mathbf{x}}^{(k)})_i = q). \end{aligned} \quad (37)$$

Finally, we observe that $\nabla f(\tilde{\mathbf{x}}^{(k)})_i \in \mathcal{W}_i^{(k)}$ implies $\nabla f(\tilde{\mathbf{x}}^{(k)})_i \neq 0$, and also $\theta_k > 0$ implies $\mathbb{E}[\nabla f(\tilde{\mathbf{x}}^{(k)})_i \tilde{d}_i^{(k)} - \frac{1}{2} L (\tilde{d}_i^{(k)})^2] > 0$, $i = 1, \dots, n$, which together with (34) implies that $\mathbb{E}[f(\tilde{\mathbf{x}}^{(k)})] > \mathbb{E}[f(\tilde{\mathbf{x}}^{(k+1)})]$. \square

Equation (37) tells us that we might observe an oscillatory or stagnating behavior when $\theta_k \leq 0$; for a detailed numerical demonstration, see Figures 3 and 4. Concerning the convergence rate obtained by SR, we prove the following bound.

Proposition 12. *Under the same assumptions of Proposition 11, if $\theta_j > 0$, $j = 0, \dots, k-1$, then*

$$\mathbb{E}[f(\tilde{\mathbf{x}}^{(k)}) - f^*] \lesssim \prod_{j=0}^{k-1} (1 - t \mu \theta_j) (f(\mathbf{x}^{(0)}) - f^*), \quad (38)$$

where $0 < 1 - t \mu \theta_j < 1$.

Proof. On the basis of (33) and (37), we have

$$\begin{aligned} & \mathbb{E}[\nabla f(\tilde{\mathbf{x}}^{(k)})_i \tilde{d}_i^{(k)} - \frac{1}{2} L (\tilde{d}_i^{(k)})^2] \\ & \geq \frac{1}{2} \theta_k \sum_{q \in \mathcal{W}_i^{(k)}} \mathbb{E}[(t \nabla f(\tilde{\mathbf{x}}^{(k)})_i + t \sigma_{1,i}^{(k)}) \nabla f(\tilde{\mathbf{x}}^{(k)})_i \mid \nabla f(\tilde{\mathbf{x}}^{(k)})_i = q] P(\nabla f(\tilde{\mathbf{x}}^{(k)})_i = q) \\ & = \frac{1}{2} \theta_k t \mathbb{E}[\nabla f(\tilde{\mathbf{x}}^{(k)})_i^2 + \nabla f(\tilde{\mathbf{x}}^{(k)})_i \sigma_{1,i}^{(k)}] \stackrel{\text{Lemma 4}}{\simeq} \frac{1}{2} \theta_k t \mathbb{E}[\nabla f(\tilde{\mathbf{x}}^{(k)})_i^2]. \end{aligned} \quad (39)$$

Substituting it into (34), we obtain

$$\begin{aligned} \mathbb{E}[f(\tilde{\mathbf{x}}^{(k+1)})] &\lesssim \mathbb{E}[f(\tilde{\mathbf{x}}^{(k)})] - \sum_{i=1}^n \frac{1}{2} \theta_k t \mathbb{E}[\nabla f(\tilde{\mathbf{x}}^{(k)})_i^2] \\ &= \mathbb{E}[f(\tilde{\mathbf{x}}^{(k)})] - \frac{1}{2} \theta_k t \mathbb{E}[\|\nabla f(\tilde{\mathbf{x}}^{(k)})\|^2]. \end{aligned}$$

Substituting (31) into it, we get

$$\mathbb{E}[f(\tilde{\mathbf{x}}^{(k+1)}) - f^*] \lesssim (1 - t\mu\theta_k) \mathbb{E}[f(\tilde{\mathbf{x}}^{(k)}) - f^*].$$

Expanding the recursion, we obtain (38). Since $\theta_j, t, \mu > 0$ we have $1 - t\mu\theta_j < 1$. Finally, $\theta_j < 2$ and $t \leq \frac{1}{L} \leq \frac{1}{2\mu}$ imply $1 - t\mu\theta_j > 0$. \square

Proposition 12 demonstrates that, under the condition $\theta_j > 0$, GD converges linearly to a neighborhood of the optimal point. Looking at (38), we see that larger values of θ_j lead to tighter bounds for the expected convergence rate of GD. Comparing (4) and (38), when $\theta_j > 1$ for many iteration steps j , it is likely to achieve a stricter bound than the one available for exact arithmetic; on the contrary, when $\theta_j < 1$ for many indices j we probably get a larger bound. Next, we prove that under the same condition as Proposition 11, the monotonicity of GD is also guaranteed when employing SR_ε for σ_2 .

Proposition 13. *Under the same assumptions of Proposition 11, but instead of using SR now σ_2 is obtained by SR_ε , if $\theta_k > 0$ in (33) then*

$$\mathbb{E}[f(\tilde{\mathbf{x}}^{(k)})] < \mathbb{E}[f(\tilde{\mathbf{x}}^{(k-1)})].$$

Proof. Denote by \mathcal{S} the finite set of values that may be taken by $t(\nabla f(\tilde{\mathbf{x}}^{(k)})_i + \sigma_{1,i}^{(k)})$. Let \mathcal{S}_1 indicate the subset of values of \mathcal{S} such that $0 < p_\varepsilon(t(\nabla f(\tilde{\mathbf{x}}^{(k)})_i + \sigma_{1,i}^{(k)})) < 1$. Analogously, we define the subsets \mathcal{S}_2 and \mathcal{S}_3 corresponding to the conditions $p_\varepsilon = 0$ and $p_\varepsilon = 1$, respectively. Finally, we introduce the quantity

$$\omega_i^{(k)} := u^{-1}(u - |t(\nabla f(\tilde{\mathbf{x}}^{(k)})_i + \sigma_{1,i}^{(k)})|).$$

Note that the numerator of $\omega_i^{(k)}$ indicates the distance of $t(\nabla f(\tilde{\mathbf{x}}^{(k)})_i + \sigma_{1,i}^{(k)})$ to u and $-u$ for $t(\nabla f(\tilde{\mathbf{x}}^{(k)})_i + \sigma_{1,i}^{(k)}) \in \mathcal{S}_2$ and $t(\nabla f(\tilde{\mathbf{x}}^{(k)})_i + \sigma_{1,i}^{(k)}) \in \mathcal{S}_3$, respectively. According to the definition of SR_ε , see (8b), when $p_\varepsilon(t(\nabla f(\tilde{\mathbf{x}}^{(k)})_i + \sigma_{1,i}^{(k)}))$ equals 0 or 1 it follows that $\omega_i^{(k)} < \varepsilon$. Further, since $t(\nabla f(\tilde{\mathbf{x}}^{(k)})_i + \sigma_{1,i}^{(k)}) \in \mathcal{S}_2$ and $t(\nabla f(\tilde{\mathbf{x}}^{(k)})_i + \sigma_{1,i}^{(k)}) \in \mathcal{S}_3$ are mutually exclusive events, we have $P(t(\nabla f(\tilde{\mathbf{x}}^{(k)})_i + \sigma_{1,i}^{(k)}) \in \{\mathcal{S}_2 \cup \mathcal{S}_3\}) = P(t(\nabla f(\tilde{\mathbf{x}}^{(k)})_i + \sigma_{1,i}^{(k)}) \in \mathcal{S}_2) + P(t(\nabla f(\tilde{\mathbf{x}}^{(k)})_i + \sigma_{1,i}^{(k)}) \in \mathcal{S}_3)$. Therefore, we define the real-valued function h as the map that associates with the random variable $\nabla f(\tilde{\mathbf{x}}^{(k)})_i + \sigma_{1,i}^{(k)}$ the quantity:

$$h(\nabla f(\tilde{\mathbf{x}}^{(k)})_i + \sigma_{1,i}^{(k)}) := \varepsilon P(t(\nabla f(\tilde{\mathbf{x}}^{(k)})_i + \sigma_{1,i}^{(k)}) \in \mathcal{S}_1) + \omega_i^{(k)} P(t(\nabla f(\tilde{\mathbf{x}}^{(k)})_i + \sigma_{1,i}^{(k)}) \in \{\mathcal{S}_2 \cup \mathcal{S}_3\}). \quad (40)$$

When $\nabla f(\tilde{\mathbf{x}}^{(k)})_i + \sigma_{1,i}^{(k)}$ is not an identically zero random variable, we have

$$\begin{aligned} \mathbb{E}[\sigma_{2,i}^{(k)} \mid \nabla f(\tilde{\mathbf{x}}^{(k)})_i, \sigma_{1,i}^{(k)}] &= u \operatorname{sign}(\nabla f(\tilde{\mathbf{x}}^{(k)})_i) (\varepsilon P(t(\nabla f(\tilde{\mathbf{x}}^{(k)})_i + \sigma_{1,i}^{(k)}) \in \mathcal{S}_1) \\ &\quad + \omega_i^{(k)} u P(t(\nabla f(\tilde{\mathbf{x}}^{(k)})_i + \sigma_{1,i}^{(k)}) \in \{\mathcal{S}_2 \cup \mathcal{S}_3\})) \\ &= u \operatorname{sign}(\nabla f(\tilde{\mathbf{x}}^{(k)})_i) h(\nabla f(\tilde{\mathbf{x}}^{(k)})_i + \sigma_{1,i}^{(k)}). \end{aligned}$$

Proceeding analogously as for (35), we obtain

$$\begin{aligned} \mathbb{E}[\nabla f(\tilde{\mathbf{x}}^{(k)})_i \tilde{d}_i^{(k)}] & \tag{41} \\ &= \sum_{q \in \mathcal{W}_i^{(k)}} \mathbb{E}[\nabla f(\tilde{\mathbf{x}}^{(k)})_i (t \nabla f(\tilde{\mathbf{x}}^{(k)})_i + t \sigma_{1,i}^{(k)}) \mid \nabla f(\tilde{\mathbf{x}}^{(k)})_i = q] P(\nabla f(\tilde{\mathbf{x}}^{(k)})_i = q) \\ &\quad + \sum_{q \in \mathcal{W}_i^{(k)}} \mathbb{E}[u \mid \nabla f(\tilde{\mathbf{x}}^{(k)})_i] h(\nabla f(\tilde{\mathbf{x}}^{(k)})_i + \sigma_{1,i}^{(k)}) \mid \nabla f(\tilde{\mathbf{x}}^{(k)})_i = q] P(\nabla f(\tilde{\mathbf{x}}^{(k)})_i = q). \end{aligned}$$

Following a similar procedure to the one obtaining (36), with SR_ε , we have

$$\begin{aligned} \mathbb{E}[(\tilde{d}_i^{(k)})^2 \mid \nabla f(\tilde{\mathbf{x}}^{(k)})_i, \sigma_{1,i}^{(k)}] &= u^2 (1 - p_\varepsilon(t \nabla f(\tilde{\mathbf{x}}^{(k)})_i + t \sigma_{1,i}^{(k)})) \\ &= (u \mid t \nabla f(\tilde{\mathbf{x}}^{(k)})_i + t \sigma_{1,i}^{(k)} \mid + \varepsilon u^2) P(\nabla f(\tilde{\mathbf{x}}^{(k)})_i + \sigma_{1,i}^{(k)} \in \mathcal{S}_1) \\ &\quad + (u \mid t \nabla f(\tilde{\mathbf{x}}^{(k)})_i + \sigma_{1,i}^{(k)} \mid + \omega_i^{(k)} u^2) P(\nabla f(\tilde{\mathbf{x}}^{(k)})_i + t \sigma_{1,i}^{(k)} \in \{\mathcal{S}_2 \cup \mathcal{S}_3\}). \\ &= u \mid t \nabla f(\tilde{\mathbf{x}}^{(k)})_i + t \sigma_{1,i}^{(k)} \mid + u^2 h(\nabla f(\tilde{\mathbf{x}}^{(k)})_i + \sigma_{1,i}^{(k)}). \end{aligned}$$

Therefore:

$$\begin{aligned} \mathbb{E}[(\tilde{d}_i^{(k)})^2] &= \sum_{q \in \mathcal{W}_i^{(k)}} \mathbb{E}[u \mid t \nabla f(\tilde{\mathbf{x}}^{(k)})_i + t \sigma_{1,i}^{(k)} \mid \mid \nabla f(\tilde{\mathbf{x}}^{(k)})_i = q] P(\nabla f(\tilde{\mathbf{x}}^{(k)})_i = q) \\ &\quad + \sum_{q \in \mathcal{W}_i^{(k)}} \mathbb{E}[u^2 h(\nabla f(\tilde{\mathbf{x}}^{(k)})_i + \sigma_{1,i}^{(k)}) \mid \nabla f(\tilde{\mathbf{x}}^{(k)})_i = q] P(\nabla f(\tilde{\mathbf{x}}^{(k)})_i = q). \end{aligned}$$

Together with (41) and in accordance with (32), we obtain

$$\begin{aligned} \mathbb{E}[\nabla f(\tilde{\mathbf{x}}^{(k)})_i \tilde{d}_i^{(k)} - \frac{1}{2} L (\tilde{d}_i^{(k)})^2] & \tag{42} \\ &= \sum_{q \in \mathcal{W}_i^{(k)}} \mathbb{E}[\nabla f(\tilde{\mathbf{x}}^{(k)})_i \tilde{d}_i^{(k)} - \frac{1}{2} L (\tilde{d}_i^{(k)})^2 \mid \nabla f(\tilde{\mathbf{x}}^{(k)})_i = q] P(\nabla f(\tilde{\mathbf{x}}^{(k)})_i = q) \\ &= \sum_{q \in \mathcal{W}_i^{(k)}} \mathbb{E}[\mid t \nabla f(\tilde{\mathbf{x}}^{(k)})_i + t \sigma_{1,i}^{(k)} \mid (\mid \nabla f(\tilde{\mathbf{x}}^{(k)})_i \mid - \frac{1}{2} L u) \mid \nabla f(\tilde{\mathbf{x}}^{(k)})_i = q] P(\nabla f(\tilde{\mathbf{x}}^{(k)})_i = q) \\ &\quad + \sum_{q \in \mathcal{W}_i^{(k)}} \mathbb{E}[(u \mid \nabla f(\tilde{\mathbf{x}}^{(k)})_i \mid - \frac{1}{2} L u^2) h(\nabla f(\tilde{\mathbf{x}}^{(k)})_i + \sigma_{1,i}^{(k)}) \mid \nabla f(\tilde{\mathbf{x}}^{(k)})_i = q] P(\nabla f(\tilde{\mathbf{x}}^{(k)})_i = q). \end{aligned}$$

The property $\theta_k > 0$ implies $\mathbb{E}[\nabla f(\tilde{\mathbf{x}}^{(k)})_i \tilde{d}_i^{(k)} - \frac{1}{2} L (\tilde{d}_i^{(k)})^2] > 0$, validating the claim. \square

Proposition 13 shows that under the same conditions as in Proposition 11, the strict monotonicity of GD can be also obtained by applying SR_ε . Further, we show that a stricter bound on convergence can be realized by utilizing SR_ε compared to that of SR. First let us define (cf. (40))

$$\beta_k := \min_{i=1,\dots,n} h(\nabla f(\tilde{\mathbf{x}}^{(k)})_i + \sigma_{1,i}^{(k)}),$$

where $\beta_k \leq \varepsilon$ for all k and define

$$\tau_2 := \min_{j=0,\dots,k} \frac{\beta_j u \mathbb{E}[\|\nabla f(\tilde{\mathbf{x}}^{(j)})\|]}{\mathbb{E}[\|\nabla f(\tilde{\mathbf{x}}^{(j)})\|^2]}. \quad (43)$$

When $\theta_k > 0$ in (33), it implies that $\mathbb{E}[\|\nabla f(\tilde{\mathbf{x}}^{(k)})\|] > \frac{1}{2} L u$. On the basis of Jensen's inequality, we get

$$\tau_2 < \frac{2\beta_j}{L} \underset{L\bar{t} \leq 1}{\leq} 2t\beta_j \leq 2t\varepsilon, \quad \text{for all } j = 1, \dots, k.$$

With (43), we may achieve a stricter bound on the convergence of GD.

Proposition 14. *Under the same assumption of Proposition 13 but instead of $t \leq \frac{1}{L}$ we have $t \leq \frac{1}{(1+2\varepsilon)L}$, if $\theta_j > 0$ in (33) for all j , then with τ_2 as in (43), we have*

$$\mathbb{E}[f(\tilde{\mathbf{x}}^{(k)}) - f^*] \lesssim \prod_{j=0}^{k-1} (1 - (t + \tau_2)\mu\theta_j) (f(\mathbf{x}^{(0)}) - f^*), \quad (44)$$

$\tau_2 \in (0, 2t\varepsilon)$ and $0 < (t + \tau_2)\mu\theta_j < 1$.

Proof. Substituting θ_k (cf. (33)) and β_k into (42), we get

$$\begin{aligned} & \mathbb{E}[\nabla f(\tilde{\mathbf{x}}^{(k)})_i \tilde{d}_i^{(k)} - \frac{1}{2} L (\tilde{d}_i^{(k)})^2] \\ & \geq \frac{1}{2} \theta_k \sum_{q \in \mathcal{W}_i^{(k)}} \mathbb{E}[(t \nabla f(\tilde{\mathbf{x}}^{(k)})_i + t \sigma_{1,i}^{(k)}) \nabla f(\tilde{\mathbf{x}}^{(k)})_i \mid \nabla f(\tilde{\mathbf{x}}^{(k)})_i = q] P(\nabla f(\tilde{\mathbf{x}}^{(k)})_i = q) \\ & \quad + \frac{1}{2} \theta_k \sum_{q \in \mathcal{W}_i^{(k)}} \mathbb{E}[\beta_k |\nabla f(\tilde{\mathbf{x}}^{(k)})_i| u \mid \nabla f(\tilde{\mathbf{x}}^{(k)})_i = q] P(\nabla f(\tilde{\mathbf{x}}^{(k)})_i = q) \\ & = \frac{1}{2} \theta_k \mathbb{E}[t \nabla f(\tilde{\mathbf{x}}^{(k)})_i^2 + t \nabla f(\tilde{\mathbf{x}}^{(k)})_i \sigma_{1,i}^{(k)} + \beta_k u |\nabla f(\tilde{\mathbf{x}}^{(k)})_i|] \\ & \simeq \frac{1}{2} \theta_k (t \mathbb{E}[\nabla f(\tilde{\mathbf{x}}^{(k)})_i^2] + \beta_k u \mathbb{E}[|\nabla f(\tilde{\mathbf{x}}^{(k)})_i|]), \quad \text{from Lemma 4.} \end{aligned} \quad (45)$$

Substituting it into (34), we obtain

$$\mathbb{E}[f(\tilde{\mathbf{x}}^{(k+1)})] \lesssim \mathbb{E}[f(\tilde{\mathbf{x}}^{(k)})] - \sum_{i=1}^n \frac{1}{2} \theta_k t \mathbb{E}[\nabla f(\tilde{\mathbf{x}}^{(k)})_i^2] - \sum_{i=1}^n \frac{1}{2} \theta_k \beta_k u \mathbb{E}[|\nabla f(\tilde{\mathbf{x}}^{(k)})_i|]$$

$$\begin{aligned}
&\leq \mathbb{E}[f(\tilde{\mathbf{x}}^{(k)})] - \frac{1}{2} \theta_k (t \mathbb{E}[\|\nabla f(\tilde{\mathbf{x}}^{(k)})\|^2] + \beta_k u \mathbb{E}[\|\nabla f(\tilde{\mathbf{x}}^{(k)})\|_1]) \\
&\leq \mathbb{E}[f(\tilde{\mathbf{x}}^{(k)})] - \frac{1}{2} \theta_k (t \mathbb{E}[\|\nabla f(\tilde{\mathbf{x}}^{(k)})\|^2] + \beta_k u \mathbb{E}[\|\nabla f(\tilde{\mathbf{x}}^{(k)})\|]). \quad (46)
\end{aligned}$$

By Jensen's inequality, we have

$$\tau_2 \leq \frac{\beta_k u \mathbb{E}[\|\nabla f(\tilde{\mathbf{x}}^{(k)})\|]}{\mathbb{E}[\|\nabla f(\tilde{\mathbf{x}}^{(k)})\|^2]} \leq \frac{\beta_k u \mathbb{E}[\|\nabla f(\tilde{\mathbf{x}}^{(k)})\|]}{\mathbb{E}[\|\nabla f(\tilde{\mathbf{x}}^{(k)})\|]^2} = \frac{\beta_k u}{\mathbb{E}[\|\nabla f(\tilde{\mathbf{x}}^{(k)})\|]}.$$

Substituting (43) into (46), we obtain

$$\mathbb{E}[f(\tilde{\mathbf{x}}^{(k+1)})] \lesssim \mathbb{E}[f(\tilde{\mathbf{x}}^{(k)})] - \frac{1}{2} \theta_k (t + \tau_2) \mathbb{E}[\|\nabla f(\tilde{\mathbf{x}}^{(k)})\|^2].$$

Substituting (31) into the right-hand side and expanding the recursion k times, we obtain the desired result with $0 < \tau_2 < 2t\varepsilon$. Furthermore, on the basis of definition of SR_ε that $0 < \varepsilon < 1$ and the property $0 < \theta_k < 2$, it is easy to check that $0 < (t + \tau_2) \mu \theta_j < 1$, which concludes the proof. \square

Similarly to SR (cf. Proposition 12), under the condition $\theta_j > 0$, the employment of SR_ε ensures linear convergence only up to a neighborhood of the optimal point. In general, Proposition 14 shows that a larger ε in SR_ε , i.e., a larger rounding bias (cf. subsection 2.2), allows for larger values of β_j and of τ_2 . Comparing (38) and (44), a larger value of τ_2 leads to a stricter bound on the convergence rate. Under the same condition as that for SR, the convergence achieved by SR_ε may be faster than that achieved by SR. These claims can be validated using numerical experiments; see, e.g., Figures 2a, 5a and 8. In the next section, we analyze the convergence behavior of GD for Case III.

4.2.3 Case III

In this case, we consider the updating rule that satisfies (21). The updating vector consists of entries $\tilde{d}_i^{(k)}$ that satisfy either (18) or (20). Our analysis demonstrates that the convergence rate is bounded between the rates observed in Case I and Case II. For the next result, we need to introduce the following quantity:

$$\alpha_k := \frac{\sum_{\mathcal{C}_2} t (\theta_k - 1) \mathbb{E}[\nabla f(\tilde{\mathbf{x}}^{(k)})_i^2]}{\mathbb{E}[\|\nabla f(\tilde{\mathbf{x}}^{(k)})\|^2]}, \quad (47)$$

where \mathcal{C}_2 (cf. (17)) is the set defined in the condition of Case III. It is easy to see that $|\alpha_k| \leq t|\theta_k - 1|$. When $0 < \theta_k < 2$ (cf. (33)), then $-t < \alpha_k < t$. Informally, α_k tends to be positive when the gradient is large (at the beginning of the process), and negative when the gradient is close to 0.

Proposition 15. *Under Assumption 1 and the condition of Case III (17), suppose that both σ_1 and σ_2 in (5) are obtained using SR with fixed stepsize t such that $t \leq \frac{1}{4L}$.*

If $\theta_j > 0$ in (33) for all j , then with α_j as in (47), we have

$$\mathbb{E}[f(\tilde{\mathbf{x}}^{(k)}) - f^*] \lesssim \prod_{j=0}^{k-1} (1 - \mu(t + \alpha_j)) (f(\mathbf{x}^{(0)}) - f^*), \quad (48)$$

and $0 < \mu(t + \alpha_j) < 1$, for $j = 0, \dots, k-1$.

Proof. Because of (21), we have

$$\begin{aligned} \mathbb{E}[f(\tilde{\mathbf{x}}^{(k+1)})] &\leq \mathbb{E}[f(\tilde{\mathbf{x}}^{(k)})] - \mathbb{E}[\nabla f(\tilde{\mathbf{x}}^{(k)})^T \tilde{\mathbf{d}}^{(k)}] + \frac{1}{2} L \mathbb{E}[\|\tilde{\mathbf{d}}^{(k)}\|^2] \\ &= \mathbb{E}[f(\tilde{\mathbf{x}}^{(k)})] - \sum_{i \in \mathcal{C}_1 \cup \mathcal{C}_2} \mathbb{E}[t \nabla f(\tilde{\mathbf{x}}^{(k)})_i^2 + t \nabla f(\tilde{\mathbf{x}}^{(k)})_i \sigma_{1,i}^{(k)} + \nabla f(\tilde{\mathbf{x}}^{(k)})_i \sigma_{2,i}^{(k)} - \frac{1}{2} L (\tilde{d}_i^{(k)})^2]. \end{aligned} \quad (49)$$

When SR is used to evaluate $\sigma_{1,i}^{(k)}$ and $\sigma_{2,i}^{(k)}$, on the basis of (29) and (39), we have

$$\begin{aligned} \mathbb{E}[f(\tilde{\mathbf{x}}^{(k+1)})] &\lesssim \mathbb{E}[f(\tilde{\mathbf{x}}^{(k)})] - \sum_{i \in \mathcal{C}_1} \frac{1}{2} t \mathbb{E}[\nabla f(\tilde{\mathbf{x}}^{(k)})_i^2] - \sum_{i \in \mathcal{C}_2} \frac{1}{2} \theta_k t \mathbb{E}[\nabla f(\tilde{\mathbf{x}}^{(k)})_i^2] \\ &= \mathbb{E}[f(\tilde{\mathbf{x}}^{(k)})] - \sum_{i=1}^n \frac{1}{2} t \mathbb{E}[\nabla f(\tilde{\mathbf{x}}^{(k)})_i^2] - \sum_{i \in \mathcal{C}_2} (\frac{1}{2} \theta_k - \frac{1}{2}) t \mathbb{E}[\nabla f(\tilde{\mathbf{x}}^{(k)})_i^2] \\ &= \mathbb{E}[f(\tilde{\mathbf{x}}^{(k)})] - \frac{1}{2} t \mathbb{E}[\|\nabla f(\tilde{\mathbf{x}}^{(k)})\|^2] - \sum_{i \in \mathcal{C}_2} \frac{1}{2} t (\theta_k - 1) \mathbb{E}[\nabla f(\tilde{\mathbf{x}}^{(k)})_i^2]. \end{aligned} \quad (50)$$

Substituting (47) into (50) and expanding the recursion k times, we obtain (48). The properties $t \leq \frac{1}{4L} \leq \frac{1}{8\mu}$ and $0 < \theta_j < 2$ imply that $1 - 2\mu t > 0$ and $-t < \alpha_j < t$, which indicates that $1 - \mu(t + \alpha_j) > 1 - 2\mu t > 0$. \square

Equation (50) can be seen as the combination of (30) with $\rho_k = 0$ and (39). From (50), it can be seen that when $0 < \theta_k < 2$, we obtain monotonicity on the objective function. When $\theta_k = 1$, we may achieve similar convergence to Case I, i.e.,

$$\mathbb{E}[f(\tilde{\mathbf{x}}^{(k+1)})] \lesssim \mathbb{E}[f(\tilde{\mathbf{x}}^{(k)})] - \frac{1}{2} t \mathbb{E}[\|\nabla f(\tilde{\mathbf{x}}^{(k)})\|^2],$$

which leads to the same convergence bound as in Corollary 10, i.e.,

$$\mathbb{E}[f(\tilde{\mathbf{x}}^{(k)}) - f^*] \lesssim (1 - t\mu)^k (f(\mathbf{x}^{(0)}) - f^*).$$

However, when $0 < \theta_k < 1$, we may obtain a negative α_k in (48), which implies a larger bound on the convergence rate than Case I. In particular, the convergence rate of (48) depends on the number of $\tilde{d}_i^{(k)} \in \mathcal{C}_2$. When $0 < \theta_k < 1$ a larger number of $\tilde{d}_i^{(k)} \in \mathcal{C}_2$ causes a smaller value of α_k (cf. (47)). On the contrary, when $\theta_k \geq 1$ a larger number of $\tilde{d}_i^{(k)} \in \mathcal{C}_2$ results in a larger value of α_k . When many $\tilde{d}_i^{(k)}$ belong to \mathcal{C}_2 and the components of the gradient vectors are close to zero (α_k is negative), we may achieve a slower convergence.

Next, we show that with SR_ε we may obtain a stricter bound on the convergence rate than that obtained by SR (cf. (48)). The proof is available in Appendix B.

Proposition 16. *Under Assumption 1 and the condition of Case III (17), suppose that σ_1 and σ_2 in (5) are obtained using SR and SR_ε , respectively, with fixed stepsize t such that $t \leq \frac{1}{4L}$. If $\theta_j > 0$ in (33) for all j , then with τ_2 as in (43), we have*

$$\mathbb{E}[f(\tilde{\mathbf{x}}^{(k)}) - f^*] \lesssim \prod_{j=0}^{k-1} (1 - \mu(t + \alpha_j + \theta_j \tau_2)) (f(\mathbf{x}^{(0)}) - f^*), \quad (51)$$

and $\tau_2 \in (0, 2t\varepsilon)$ with the values α_j defined in (47).

Again, with SR_ε , we obtain a stricter bound on the convergence rate than that obtained by SR under Case III (comparing (48) and (51)). This comparison shows that a faster convergence may be obtained when using SR_ε in place of SR for σ_2 . Equation (51) shows that the convergence bound obtained by SR_ε depends on the values of ε and t . Therefore, a larger ε in SR_ε or a larger t can result in faster convergence.

In the next section, we compare our convergence analysis of GD using fixed-point arithmetic to that using floating-point arithmetic.

5 Comparison with floating-point arithmetic

In this section, we demonstrate the different behaviors of our rounding method SR_ε in fixed-point and floating-point arithmetic. When using SR_ε to implement GD in fixed-point arithmetic, the rounding bias on each entry of iterate is in the same scale (u). However, in floating-point arithmetic, owing to the fact that numbers are not uniformly distributed, the rounding bias on each entry of the iterate also exhibits the same behavior. In particular, when implementing GD with limited precision in floating-point arithmetic, using SR_ε , the updating stepsize is adaptive to the entries of each iterate.

Now let us dive into the difference between fixed-point and floating-point computation for different rounding methods. We start by comparing their expressions of the updating vector $\tilde{\mathbf{d}}^{(k)}$ of GD in fixed-point and floating-point number formats. In accordance with the argument in [19, Sec. 4.2] that the small numbers can be represented by the subnormal numbers in floating-point number formats, therefore stagnation of GD happens when evaluating the subtraction in (3). However, the stagnation of GD happens when evaluating the multiplication of t and gradients in fixed-point number formats. To have a clear observation, we assume that stagnation starts from the k th iteration step and all the computations before stagnation are exact (errors are negligible) for both fixed-point and floating-point arithmetic, i.e., $\text{fi}(\nabla f(\mathbf{x}^{(k)})) = \nabla f(\mathbf{x}^{(k)})$ and $\text{fl}(t \text{fl}(\nabla f(\mathbf{x}^{(k)}))) = t \nabla f(\mathbf{x}^{(k)})$ for fixed-point and floating-point arithmetic, where $\text{fl}(\cdot)$ denotes a general rounding operator that converts a real number $x \in \mathbb{R}$ to the floating-point number representation \hat{x} .

When GD stagnates with RN for the i th coordinate of $\mathbf{x}^{(k)}$ and $\tilde{d}_i^{(k)} \neq 0$, we have a fixed magnitude of $\tilde{d}_i^{(k)}$ using stochastic rounding for fixed-point number

representation, given by

$$\tilde{d}_i^{(k)} = u \operatorname{sign}(\nabla f(\mathbf{x}^{(k)})_i).$$

Under the same assumption, we have an adaptive magnitude of $\tilde{d}_i^{(k)}$ using stochastic rounding methods for floating-point number representation. On the grounds of the model of floating-point operation [15, (2.4)], we have the following value for $\tilde{d}_i^{(k)}$:

$$\tilde{d}_i^{(k)} = \begin{cases} \operatorname{sign}(\nabla f(\mathbf{x}^{(k)})_i) |x_i^{(k)}| \delta_i^{(k)} + t \nabla f(\mathbf{x}^{(k)})_i (1 - \delta_i^{(k)}), & \text{if } \operatorname{sign}(x_i^{(k)} \nabla f(\mathbf{x}^{(k)})_i) = 1, \\ \operatorname{sign}(\nabla f(\mathbf{x}^{(k)})_i) |x_i^{(k)}| \delta_i^{(k)} + t \nabla f(\mathbf{x}^{(k)})_i (1 + \delta_i^{(k)}), & \text{if } \operatorname{sign}(x_i^{(k)} \nabla f(\mathbf{x}^{(k)})_i) = -1, \end{cases} \quad (52)$$

where $0 < \delta_i^{(k)} < 2u$ denotes the relative error caused by evaluating $x_i^{(k)} - t \nabla f(\mathbf{x}^{(k)})_i$ using stochastic rounding methods. For different stochastic rounding methods, $\tilde{d}_i^{(k)}$ may be either zero or one of the expressions in (52) with different probability distributions. Therefore, GD behaves differently with different rounding methods and number representations.

Now let us study the difference between different rounding methods in each number representation. For fixed-point arithmetic, we obtain the following updating vectors of GD when using SR and SR_ε .

Proposition 17. *Assume the use of fixed-point arithmetic to implement GD, and that $\text{RN}(\tilde{d}_i^{(k)}) = 0$ for the i th component in $\tilde{\mathbf{d}}^{(k)}$, i.e., $|t \nabla f(\mathbf{x}^{(k)})_i| < \frac{1}{2}u$. If $\text{fl}(\nabla f(\mathbf{x}^{(k)})) = \nabla f(\mathbf{x}^{(k)})$, then for SR we have*

$$\mathbb{E}[\tilde{d}_i^{(k)} \mid t \nabla f(\tilde{\mathbf{x}}^{(k)})_i] = t \nabla f(\tilde{\mathbf{x}}^{(k)})_i, \quad (53)$$

and for SR_ε we have

$$\mathbb{E}[\tilde{d}_i^{(k)} \mid t \nabla f(\mathbf{x}^{(k)})_i] = \begin{cases} u \operatorname{sign}(\nabla f(\mathbf{x}^{(k)})_i), & \text{if } \varepsilon \geq 1 - \frac{|t \nabla f(\mathbf{x}^{(k)})_i|}{u}, \\ t \nabla f(\mathbf{x}^{(k)})_i + \varepsilon u \operatorname{sign}(\nabla f(\mathbf{x}^{(k)})_i), & \text{otherwise.} \end{cases}$$

The proof is available in Appendix B. From Proposition 17, we observe that SR and SR_ε result in an average updating magnitude of GD that is similar to and slightly larger than that in exact computation, respectively. In fixed-point arithmetic, the updating length of GD is independent of its iterate $\mathbf{x}^{(k)}$ for both SR and SR_ε . Additionally, the rounding bias introduced by SR_ε only depends on u and has the same sign vector as its gradient.

In floating-point arithmetic, signed- SR_ε and SR_ε generate the same magnitude of rounding bias but the rounding bias may have a different sign. When GD stagnates with RN, we observe the following properties of the updating magnitudes of GD when using SR and signed- SR_ε .

Proposition 18. *Assume the use of floating-point arithmetic to implement GD, and that $\text{RN}(x_i^{(k)} - \tilde{d}_i^{(k)}) = x_i^{(k)}$, i.e., $|\frac{t \nabla f(\mathbf{x}^{(k)})_i}{x_i^{(k)}}| < u$. If $\text{fl}(t \text{fl}(\nabla f(\mathbf{x}^{(k)}))) = t \nabla f(\mathbf{x}^{(k)})$, then for SR we have*

$$\mathbb{E}[\tilde{d}_i^{(k)} \mid x_i^{(k)} - t \nabla f(\mathbf{x}^{(k)})_i] = t \nabla f(\tilde{\mathbf{x}}^{(k)})_i, \quad (54)$$

and for signed-SR $_{\varepsilon}$, when $0 < p_{\varepsilon s} < 1$, we have

$$\begin{aligned} & \mathbb{E}[\tilde{d}_i^{(k)} \mid x_i^{(k)} - t \nabla f(\mathbf{x}^{(k)})_i] \\ &= \begin{cases} (1 + \varepsilon + \varepsilon \delta_i^{(k)}) t \nabla f(\mathbf{x}^{(k)})_i + \text{sign}(\nabla f(\mathbf{x}^{(k)})_i) |x_i^{(k)}| \varepsilon \delta_i^{(k)}, & \text{if } \text{sign}(x_i^{(k)} \nabla f(\mathbf{x}^{(k)})_i) = -1, \\ (1 + \varepsilon - \varepsilon \delta_i^{(k)}) t \nabla f(\mathbf{x}^{(k)})_i + \text{sign}(\nabla f(\mathbf{x}^{(k)})_i) |x_i^{(k)}| \varepsilon \delta_i^{(k)}, & \text{if } \text{sign}(x_i^{(k)} \nabla f(\mathbf{x}^{(k)})_i) = 1, \end{cases} \end{aligned} \quad (55)$$

where $0 < \delta_i^{(k)} < 2u$.

The proof is available in Appendix B. Since $t \nabla f(\mathbf{x}^{(k)})_i$ is relatively small compared to $x_i^{(k)}$ in Proposition 18, the magnitude of $\tilde{d}_i^{(k)}$ is significantly affected by $|x_i^{(k)}|$. Consequently, $\mathbb{E}[\tilde{d}_i^{(k)} \mid x_i^{(k)} - t \nabla f(\mathbf{x}^{(k)})_i]$ automatically adapts to the scale of $x_i^{(k)}$ for each entry of $\mathbf{x}^{(k)}$ by using signed-SR $_{\varepsilon}$ in floating-point arithmetic, whereas this adaptivity does not hold for SR. Comparing Propositions 17 and 18, the magnitude of the updating vector of GD is independent of u or the current iterate when using SR in both fixed-point and floating-point arithmetic. In particular, when GD stagnates with RN, SR may lead to a similar convergence behavior to exact computation on average. This means using a uniform stepsize t for each entry of $\mathbf{x}^{(k)}$. However, when using signed-SR $_{\varepsilon}$, the convergence speed mainly depends on the magnitude of the iterate of GD in floating-point arithmetic and is largely improved by the adaptive rounding bias along each coordinate of $\mathbf{x}^{(k)}$, while the updating magnitude of GD is almost consistent along each coordinate of $\mathbf{x}^{(k)}$ in fixed-point number representation.

In general, SR performs similarly in both floating-point and fixed-point arithmetic. SR $_{\varepsilon}$ and signed-SR $_{\varepsilon}$ have a better effect than SR on both floating-point and fixed-point arithmetic. Thanks to the non-uniform distributed number representation in floating-point arithmetic, the rounding bias caused by SR $_{\varepsilon}$ and signed-SR $_{\varepsilon}$ is also non-uniform, which results in a faster convergence than that of GD in exact arithmetic. For fixed-point arithmetic, the rounding bias caused by SR $_{\varepsilon}$ is also uniform as its number distribution, which may have a less obvious advantage in accelerating GD than in floating-point arithmetic. Despite the fact that floating-point number representation has a wider number representation owing to the non-uniform distributed number representation, many practical low-cost embedded microprocessors and microcontrollers (e.g., FPGA designs) are limited to finite-precision signal processing using fixed-point arithmetic due to the cost and complexity of floating-point hardware. In both number representations, the implementation of GD using SR $_{\varepsilon}$ shows better performance compared to SR.

6 Simulation studies

In this section, we validate our theoretical results by applying GD with limited-precision number formats on several case studies: a quadratic problem, the two-dimensional Rosenbrock's function, Himmelblau's function, a binary logistic regression model (BLR), and a four-layer fully connected NN. We numerically show that Rosenbrock's function satisfies the PL condition in a certain domain and achieves linear convergence of GD. Himmelblau's function is used to demonstrate that by using stochastic rounding, GD can converge exactly to the optimal point instead of a nearby neighborhood. BLR is proven to satisfy the PL condition by [10], and we validate our theoretical results by training a BLR using different rounding methods and learning

stepsizes. Finally, we test the convergence of GD on training a four-layer NN and show that, despite this example not satisfying the PL condition, the numerical results are similar to those observed in the other experiments.

As discussed in subsection 3.3, the stagnation of GD is normally caused by σ_2 in (5). Therefore, for each simulation study, we employ two different number formats: one for evaluating σ_2 and the other for the working precision, where all the other operations are implemented using this working precision. Note that in all case studies, apart from the four-layer NN, we use low-precision fixed-point number formats, with their implementation relying on the Matlab fi toolbox. Due to the slow computation speed of fi toolbox, in the four-layer NN case, we only evaluate σ_2 with limited-precision fixed-point numbers and use single-precision computations for the other operations. Note that selecting the best number format for a procedure that relies on fixed-point arithmetic operations is problem-dependent and, to the authors' knowledge, there is no systemic way to select a priori the best number format for a given problem. In the preprocessing procedure, we test various values for QI and QF in different case studies. For convenience, the values of the QI are chosen to prevent overflow problems for the case studies like Quadratic, Rosenbrock, and Himmelblau functions. For more challenging examples like BLR and Four-layer NN, we choose the number of integers in such a way that it provides a similar result to that of single-precision computation. Nevertheless, Overflow is generally less critical than underflow when considering the vanishing gradients problem. Here, we focus on showing that the vanishing gradient problems can be eliminated by the use of stochastic rounding methods. The selected values of QI are reported in Table 2.

The considered values for QF are taken as small as possible in such a way that it allows us to easily observe the influence of rounding errors and validate our theoretical results. We start by setting u to 2^{-12} , and then we increase or decrease u until we achieve the largest value of u that guarantees the convergence. The considered number formats are summarized in Table 2. Additionally, the starting point $\mathbf{x}^{(0)}$ for all the numerical studies in this section is chosen as either: (1) integers that can be exactly represented in the designed fixed-point arithmetic, e.g., Quadratic, Rosenbrock, and Himmelblau functions, or (2) a rounded version of the original starting point obtained using the rounding to the nearest method, e.g., BLR and the four-layer fully connected NN where the MNIST data are normalized. In the latter case, the rounded $\mathbf{x}^{(0)}$ serves as the starting point for GD, and different rounding methods are then applied to study their impact on the convergence of the algorithm.

Table 2 Number formats of fixed-point representation for different case studies. The third column indicates how the multiplication $t \nabla f(\mathbf{x}_k)$ is carried out.

Case study	Working precision	Multiplication
Quadratic	Q26.6 ($u = 2^{-6}$)	Q26.6 ($u = 2^{-6}$)
Rosenbrock	Q8.10 ($u = 2^{-10}$)	Q12.6 ($u = 2^{-6}$)
Himmelblau	Q8.8 ($u = 2^{-8}$)	Q8.8 ($u = 2^{-8}$)
BLR	Q15.8 ($u = 2^{-8}$)	Q15.8 ($u = 2^{-8}$) and Q15.6 ($u = 2^{-6}$)
Four-layer NN	Binary32 ($u = 2^{-23}$)	Q8.8 ($u = 2^{-8}$)

For the cases of Rosenbrock’s function and NN, we also compare the performances of low-precision fixed-point computation with those of low-precision floating-point computation. For all the simulation studies, we compare the results obtained by SR and SR_ε to those obtained by RN. The baselines are obtained by single-precision (Binary32) floating-point computation with RN. We remark that there is a huge difference between the magnitude of the machine precision of single precision (2^{-23}) and those of other fixed-point number formats, which stay above 2^{-10} . Therefore, we look at the comparison with the baselines as a surrogate of a comparison with exact arithmetic.

6.1 Quadratic problems

In section 5, we have demonstrated that SR performs very similarly in fixed-point and floating-point arithmetic, yet signed- SR_ε and SR_ε have a positive impact on floating-point arithmetic and a modestly positive impact on fixed-point arithmetic. To better understand this phenomenon, let us compare the convergence behavior of GD using different rounding methods with fixed-point and floating-point arithmetic. For instance, when optimizing a least-squares problem of the form $F_1(\mathbf{x}) = \frac{1}{2}(\mathbf{x} - \mathbf{x}^*)^T A(\mathbf{x} - \mathbf{x}^*)$, where $A = \text{diag}(100, 10, 10^{-3}, 10^{-3}, 10^{-3})$ and $\mathbf{x}^* = [10^{-1}, 1, 10, 100, 1000]^T$, so that the entries of \mathbf{x}^* are of different scales. When using fixed-point arithmetic, the rounding bias introduced by SR_ε can not take care of the scale of each entry of \mathbf{x}^* , but it can be done when using SR_ε in floating-point arithmetic. To achieve a descent updating direction, we employ signed- SR_ε [19, Def. 2.3] in floating-point arithmetic to customize the sign of the rounding bias.

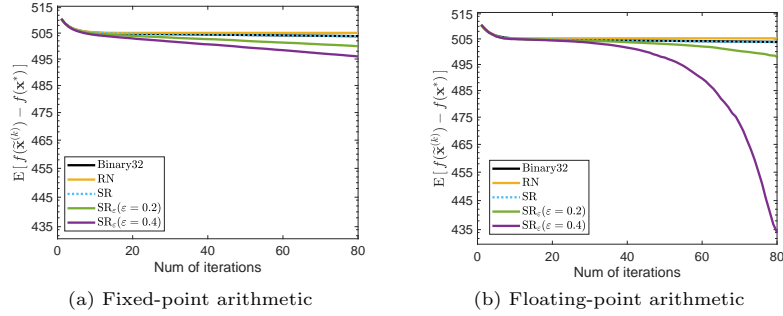


Fig. 2 A quadratic problem: comparison of the objective values using different rounding scheme with fixed-point arithmetic (Q26.6) (a) and floating-point arithmetic (8 bits with 3 significant bits) (b); settings: stepsize $t = 2^{-6}$ and $\mathbf{x}^* = [10^{-1}, 1, 10, 100, 1000]^T \in \mathbb{R}^5$.

Figure 2 shows the comparison of objective values when optimizing F_1 using GD with different rounding schemes using fixed-point arithmetic (Figure 2a) and floating-point arithmetic (Figure 2b). Due to the overlapping between the results of SR and Binary32, we utilize a dashed line for SR (only) in Figure 2 for readability. For both figures, the baseline is obtained by optimizing F_1 using single-precision (32-bit) computation and RN. In Figure 2a, both σ_1 and σ_2 are obtained using the same rounding

scheme. For instance, the yellow line in Figure 2a shows that both σ_1 and σ_2 are obtained using RN with fixed-point number representation Q26.6. In Figure 2b, we apply 8-bit floating-point computation with 3 significant bits. Comparing Figures 2a and 2b, it can be observed that the convergence rates of GD using RN and SR are very similar in fixed-point and floating-point number formats. However, SR_ε has extraordinarily different performance in these two number formats. Figure 2a suggests that in fixed-point arithmetic, GD with the accumulated rounding bias in the descent direction maintains a linear convergence rate but with a smaller base compared to exact computation. On the other hand, using SR_ε in floating-point arithmetic appears to yield an almost superlinear convergence rate.

To better understand how θ_k (33) influences the convergence of GD with the employment of SR (Proposition 11) and SR_ε (Proposition 13), let us compare the convergence behavior of GD using different rounding precisions. As an example, consider the optimization of a least-squares problem represented by $F_4(\mathbf{x}) = \frac{1}{2}(\mathbf{x} - \mathbf{x}^*)^T A(\mathbf{x} - \mathbf{x}^*)$, where $A = \text{diag}(1, 1, 10^{-3}, 10^{-3}, 10^{-3})$ and $\mathbf{x}^* = [1000, 100, 10, 100, 1000]^T$. This particular problem formulation is significant as it captures scenarios where the elements of \mathbf{x}^* exhibit different scales and the choice of A prevents L from being excessively large, which prevents θ_k from becoming consistently negative. To obtain an approximation of θ_k , we replace the sets $\mathcal{W}_i^{(k)}$ in (33) with the gradient entries at the k th step, encountered across the various simulations, and we set $L = 1$.

Figure 3 shows the approximation of θ_k (Figure 3a) and the value of $\text{E}[f(\mathbf{x}^{(k+1)}) - f(\mathbf{x}^{(k)})]$ (Figure 3b) over 40 simulations using fixed-point arithmetic with $u = 2^{-4}$. Note that Figure 3b is plotted on a logarithmic scale, with an additional offset of 10^{-16} added to the data. It can be seen that θ_k is always negative due to the large rounding precision u , which in turn causes $\text{E}[f(\mathbf{x}^{(k+1)})] = \text{E}[f(\mathbf{x}^{(k)})]$ for some iteration with the utilization of SR, i.e., stagnation of GD. This observation is consistent with the discussion after (33) and Proposition 11, i.e., a negative θ_k may lead to stagnation or oscillation of GD. Furthermore, the employment of SR_ε appears to guarantee the strict monotonicity of $\text{E}[f(\mathbf{x}^{(k)})]$ even if θ_k is negative. This phenomenon occurs because the definition of θ_k considers the smallest possible value of the gradient entries. As discussed after (33), these small gradients can be compensated by the expected rounding errors intentionally designed in the descent direction when applying SR_ε . By increasing the rounding precision to $u = 2^{-6}$, the results presented in Figure 4 show that θ_k remains consistently positive throughout the optimization process, with only a few exceptions in the last 10 iteration steps. Additionally, it shows that $\text{E}[f(\mathbf{x}^{(k+1)}) - f(\mathbf{x}^{(k)})]$ is always positive for both SR and SR_ε , indicating a strict monotonicity of the objective function. Overall, these observations validate Propositions 11 and 13, which highlight the strict monotonicity properties associated with the sign of θ_k .

6.2 Rosenbrock's function

Rosenbrock's function is a non-convex function, characterized by a wide almost flat valley around its optimum; it is defined as $F_2(\mathbf{x}) = (1 - x_1)^2 + 100(x_2 - x_1^2)^2$. Although it does not satisfy (2) for all \mathbf{x} , it can be numerically checked that Rosenbrock's function satisfies (1) and (2) with $L = 2610$ and $\mu = 0.2$ for $\mathbf{x} \in [0, 2]^2$.

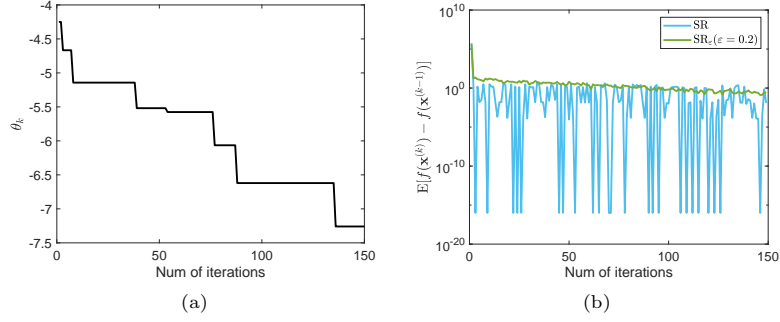


Fig. 3 Approximation of θ_k (a) and $E[f(\mathbf{x}^{(k+1)}) - f(\mathbf{x}^{(k)})]$ (b) over 40 simulations using different rounding schemes with fixed-point arithmetic (Q28.4); settings: stepsize $t = 1$ and $\mathbf{x}^{(0)} = \mathbf{0} \in \mathbb{R}^5$.

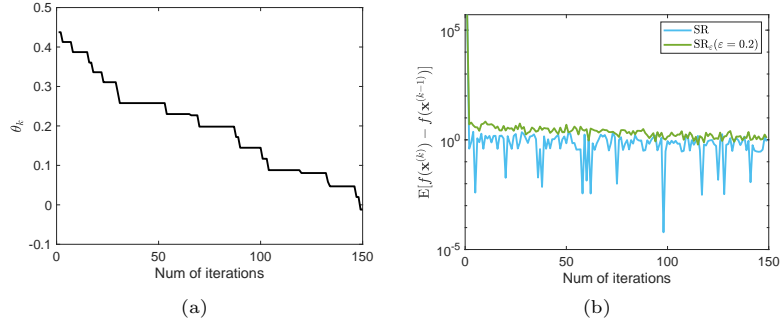


Fig. 4 Approximation of θ_k (a) and $E[f(\mathbf{x}^{(k+1)}) - f(\mathbf{x}^{(k)})]$ (b) over 40 simulations using different rounding schemes with fixed-point arithmetic (Q26.6); settings: stepsize $t = 1$ and $\mathbf{x}^{(0)} = \mathbf{0} \in \mathbb{R}^5$.

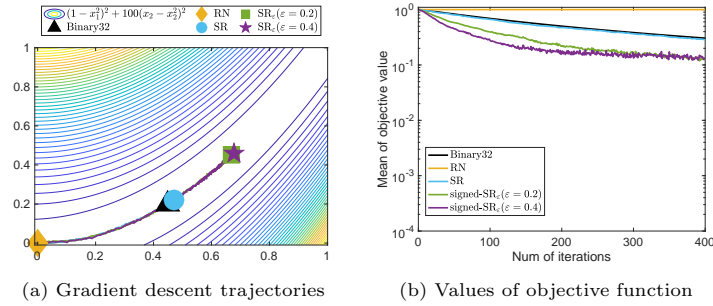


Fig. 5 Rosenbrock's function in two dimensions: comparison of the gradient descent trajectories (a) and of the correspondent objective values (b); settings: stepsize $t = 2^{-10}$ and Q12.6 for evaluating the multiplication of t and gradient and Q8.10 for the remaining operations.

Figure 5 shows the trajectories (Figure 5a) and the corresponding means of objective function evaluations over 30 simulations (Figure 5b) when implementing GD with fixed-point numbers formats and different rounding schemes. The endpoints of GD

obtained by different rounding methods are represented by distinct shapes, e.g., a triangle for single-precision computation, a diamond for RN, a circle for SR, a square for $\text{SR}_\varepsilon(\varepsilon = 0.2)$, and a pentagram for $\text{SR}_\varepsilon(\varepsilon = 0.4)$. To better observe the influence of rounding errors on the convergence of GD, we apply low precision to compute the multiplication of t and the gradients (Q12.6) and higher precision for the remaining operations to maintain the accuracy (Q8.10). The starting point is $\mathbf{x}^{(0)} = [0, 0]^T$. It can be seen from Figure 5a that GD relying on RN stagnates quite early because of the loss of gradient information. SR follows a very similar convergence to the baseline that validates Corollary 10. When using SR_ε , increasing the value of ε leads to a faster convergence to the optimum, which matches the conclusion in Theorem 9 and Propositions 14 and 16. Furthermore, from Figure 5b, with $\varepsilon = 0.4$, the mean of the objective value at the 64th iteration is similar to that obtained by single-precision at the 400th iteration, i.e., 0.31. Due to the wide valley in Rosenbrock’s function, a small deviation can cause a large oscillation in the objective function. Therefore, the small rounding bias introduced by SR_ε will result in oscillations in the objective function’s values.

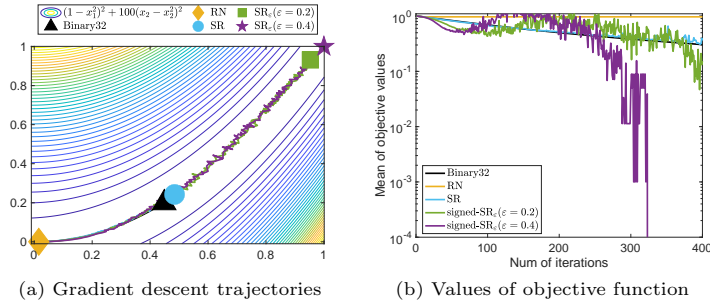


Fig. 6 Rosenbrock’s function in two dimensions: comparison of the gradient descent trajectories (a) and of the correspondent objective values (b); settings: stepsize $t = 2^{-10}$ and Binary8 [19, Sec. 2.1] with 3 significant bits.

Further, we repeat the same simulation study with an 8-bit floating-point number format with 3 significant digits. Figure 6 shows the trajectories and the corresponding mean of objective function evaluations when different rounding methods are employed in floating-point arithmetic. Note that signed- SR_ε introduces rounding biases with the same magnitudes as those obtained by SR_ε . From Figure 6, it can be observed that RN causes stagnation of GD, and SR follows a similar trajectory to that obtained by single-precision computation. Signed- SR_ε significantly accelerates the convergence of GD due to the expected rounding errors in the descent direction. When $\varepsilon = 0.4$, despite the presence of oscillations in the mean of objective function values, GD converges to the optimum within a maximum of 324 iterations for all 30 simulations.

6.3 Himmelblau’s function

Now, in line with the discussion in subsection 3.1, we show with an illustrative example that when the optimal point \mathbf{x}^* can be represented exactly in the available number format, we have that $\|\tilde{\mathbf{x}}^{(k)} - \mathbf{x}^*\| \rightarrow 0$. On the other hand, when \mathbf{x}^* cannot be represented exactly, GD converges to a neighborhood around \mathbf{x}^* . The size of this neighborhood is determined by the value of u . Let us consider the minimization of Himmelblau’s function $F_3(\mathbf{x}) = (x_1^2 + x_2 - 11)^2 + (x_1 + x_2^2 - 7)^2$, using single-precision computation and fixed-point number representation with Q8.8. We remark that Himmelblau’s function does not satisfy the PL condition for all x , but this is inconsequential for this test. The function f has four global minimizers \mathbf{x}_i^* , for $i = 1, \dots, 4$, known in closed form. In particular, we focus on scenarios where GD converges towards two distinct points: $\mathbf{x}_1^* = [3, 2]^T$, which is exactly representable, and $\mathbf{x}_4^* = [3.584428, -1.848126]^T$, which is not exactly representable. In Figure 7 we report the averaged objective function values (over 40 runs) for different rounding schemes, i.e., RN, SR, and SR_ε . As anticipated, when the starting point is close to $\mathbf{x}_4^* = [3.584428, -1.848126]^T$, all the rounding methods can only guide GD to a neighborhood around \mathbf{x}_4^* . When GD converges to $\mathbf{x}_1^* = [3, 2]^T$, all the stochastic rounding methods retrieve the exact value \mathbf{x}_1^* . However, RN causes GD to stagnate due to the problem of vanishing gradient. Additionally, in the context of utilizing SR to achieve convergence to \mathbf{x}_1^* , Figure 7d shows the number of gradient components satisfying (15). It can be seen that with the progression of iteration steps, the number of gradient components satisfying (15) gradually decreases. This trend suggests a transition in the updating process, first from Case I to Case III, and finally to Case II, aligning with the discussion after (5).

6.4 Binary logistic regression

Let us study the impact of rounding errors on solving logistic regression problems. Logistic regression is commonly used to solve binary classification problems and is proven to satisfy the PL condition by [10] over any compact set. We use BLR to classify the handwritten digits 3 and 8 in the MNIST database. As in [2], the pixel values are normalized to $[0, 1]$. The default decision threshold is set at 0.5 for interpreting probabilities to class labels since the sample class sizes are almost equal [33]. Specifically, class 1 is defined for those predicted scores larger than or equal to 0.5.

We study the convergence of GD with different rounding precisions. For each simulation study, we demonstrate two rounding precisions, i.e., the working precision and the precision for evaluating σ_2 . Figure 8 shows the comparison of the BLR’s testing errors, obtained by the various rounding methods. In Figure 8a, we employ enough digits (Q15.8) so that GD has no stagnation utilizing RN. It can be observed that SR and RN yield very similar results, while SR_ε leads to faster convergence of GD compared to RN and SR with the same rounding precision. Additionally, increasing the value of ε results in a faster convergence of GD. Keeping the same working precision and lowering the precision in evaluating σ_2 , we observe the stagnation of GD with RN and that SR provides a very similar result to the one shown in Figure 8a; for more details see Figure 8b. In the same figure, SR_ε utilizes the large rounding errors and leads to a significantly faster convergence rate of GD than the one shown in Figure 8a.

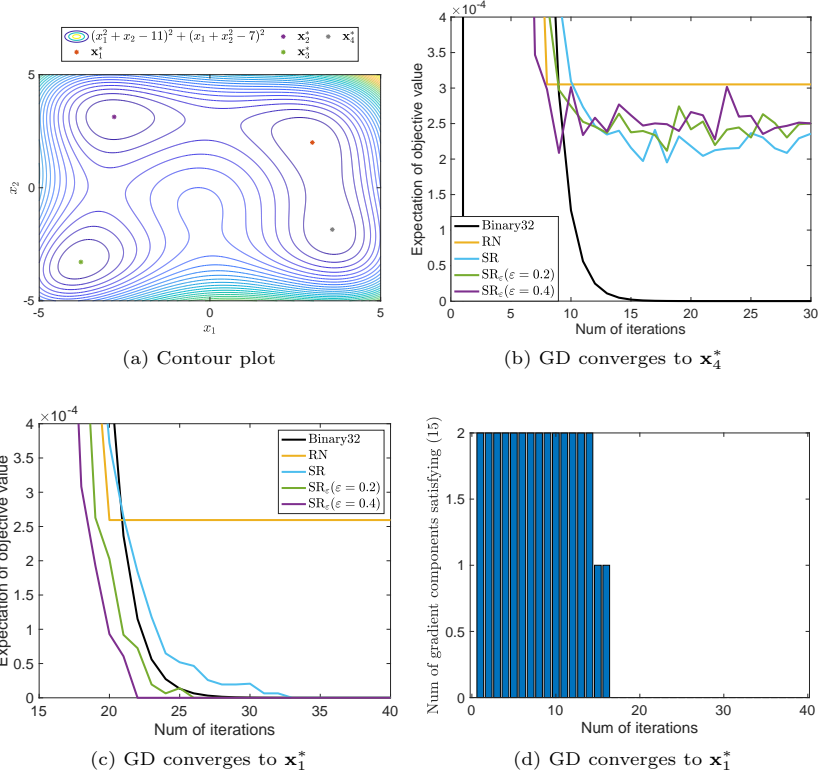


Fig. 7 Himmelblau's Function implemented using with stepsize $t = 0.012$ and fixed-point numbers Q8.8: contour plot with the 4 global minimizers \mathbf{x}_i^* , with $i = 1, \dots, 4$ (a), comparison of the objective values when GD converges to \mathbf{x}_4^* (b) and comparison of the objective values when GD converges to \mathbf{x}_1^* (c); Number of gradient components satisfying (15) when GD converges to \mathbf{x}_1^* using SR.

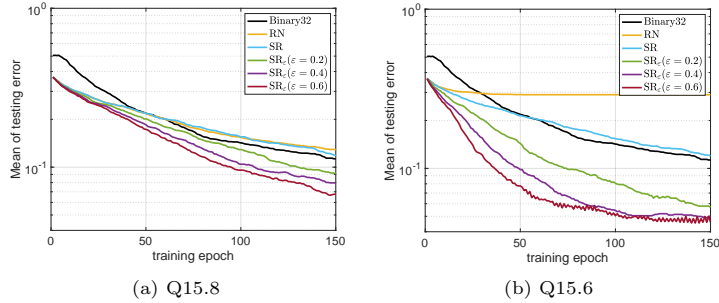


Fig. 8 Mean of objective values over 10 simulations of BLR with stepsize $t = 0.1$ (0.1015625 in Q15.8) between RN, SR and SR_ε with $\varepsilon = 0.2$, $\varepsilon = 0.4$ and $\varepsilon = 0.6$ with working precision Q15.8 and the precision for evaluating σ_2 , i.e., Q15.8 (a) and Q15.6 (b).

Again, a faster convergence of GD can be obtained by increasing the value of ε . However, comparing Figures 8a and 8b, it can be seen that when the rounding precision

and ε are both large, oscillations may occur as GD approaches the global optimum. For an example, see the result of SR_ε with $\varepsilon = 0.6$ in Figure 8b.

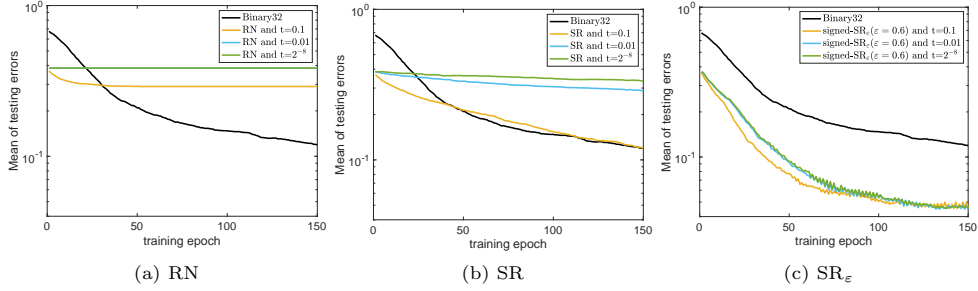


Fig. 9 Mean of objective values over 10 simulations with working precision Q15.8, precision for evaluating σ_2 Q15.6, and different stepsize 0.1 (0.1015625 in Q15.8), 0.01 (0.01171875 in Q15.8) and the smallest number that can be represented in Q15.8, i.e., $2^{-8} \approx 0.004$, for RN (a), SR (b), and SR_ε (c).

Next, we study the influence of the stepsize t in (5) on the convergence of GD with low-precision computation for different rounding methods. We employ the same number format as in Figure 8b and we vary the stepsize of GD. In particular, we consider $t = 0.1, 0.01$ and the smallest number that can be represented in Q15.8, i.e., $2^{-8} \approx 0.004$ for each rounding method such as RN, SR, and SR_ε with $\varepsilon = 0.6$. Figure 9 shows the results obtained using the different values of t and rounding schemes. From Figure 9a, it can be seen that decreasing the value of t makes GD stagnate earlier with RN. When SR is employed (cf. Figure 9b), the convergence rate is significantly more sensitive to the value of t . When employing SR, a small value of t leads to a slower convergence rate. When t is relatively small, e.g., $t = 2^{-8}$, GD almost stagnates with SR; see Figure 9b. However, it can be observed that the convergence rate obtained using SR_ε is hardly affected by the stepsize when $t \leq 0.1$. In general, both RN and SR are sensitive to t , while SR_ε is less sensitive to t due to the parameter ε in (8a). When t is small, the probability of rounding numbers towards 0 in SR (cf. (7)) is close to 1, while it is dominated by $1 - \varepsilon$ in SR_ε (cf. (8a)). Therefore, an almost constant rounding probability is achieved in SR_ε , which makes SR_ε less sensitive to the value of t when implementing GD in a low-precision number format.

6.5 Four-layer fully connected NN

Now we show that our theoretical conclusion for problems satisfying the PL condition is also applicable for the training of a four-layer fully connected NN. In particular, the convergence rate of GD with SR_ε is faster than that with SR, although the PL condition does not hold here. The latter property is showcased for both fixed-point and floating-point representation systems. The NN is trained to classify the 10 handwritten digits (from 0 to 9) in the MNIST database. Again, the pixel values are normalized to $[0, 1]$. The NN is built with the ReLU activation function in the hidden layer and the softmax activation function in the output layer. The hidden layers contain 512,

256, and 128 units. In the backward propagation, the cross-entropy loss function is optimized using GD. The weights matrix is initialized using Xavier initialization [34] and the bias is initialized as a zero vector.

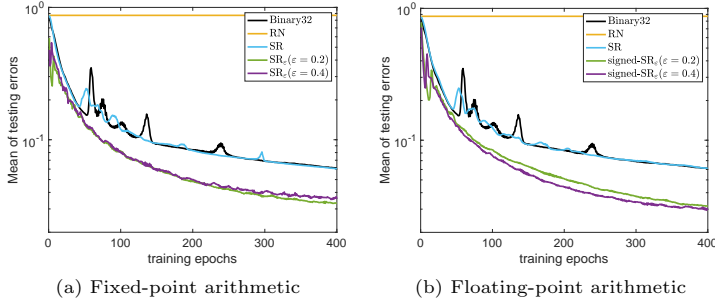


Fig. 10 Mean of testing errors of the NN trained over 10 simulations using fixed-point number format Q8.8 (a) and using Binary16 with 5 significant digits (b).

Figure 10a shows the means of testing errors of the NNs trained using Binary32 for working precision and Q8.8 for evaluating σ_2 with different rounding methods, such as RN, SR, and SR_ϵ . Again, RN causes the stagnation of GD due to the problem of vanishing gradient. SR results in a very similar testing error to single-precision computation. The testing error is around 0.06 with 400 iterations of GD using SR and single-precision computation, while a similar accuracy can be achieved by SR_ϵ with around 150 iterations. Comparing the results of SR_ϵ with $\epsilon = 0.2$ and $\epsilon = 0.4$, slightly larger oscillations are gained with a larger value of ϵ . Overall, SR_ϵ with $\epsilon = 0.2$ leads to a slightly lower testing error than SR_ϵ with $\epsilon = 0.4$. Next, we repeat the simulations with a 16-bit floating-point number format with 5 significant digits using different rounding methods. From Figure 10b, it can be seen that the results are very similar to that of fixed-point number formats. Comparing Figure 10a and Figure 10b, the outcomes obtained using SR_ϵ with a floating-point number format demonstrate a slight improvement over those achieved with a fixed-point number format, although the significance of this improvement is negligible. Additionally, for a large number of layers, it may be beneficial to use SR for evaluating computations such as inner products as it typically reduces the magnitude of rounding errors, and it is unbiased. The use of biased stochastic rounding such as SR_ϵ is recommended for evaluating the multiplication of the learning rate with the rounded gradient as it prevents the vanishing gradient problem. In the situation where the rounding errors are significant, for instance because of a large dimension n , one may need to tune u or t to restore the monotonicity of GD. In such a case, if the sign of the rounded gradient corresponds to that of the true gradient, then a smaller stepsize t should be sufficient. Otherwise, we recommend to use higher precision (i.e., smaller u).

In general, when the convergence of GD is guaranteed, low-precision computation can result in a faster convergence rate compared to higher precision when using SR_ϵ ; see Figures 5, 8 and 10. With low-precision computation, the utilization of SR yields results of GD that are similar to those obtained by the exact computation, and the

use of RN may result in stagnation of GD. Additionally, the performance of SR is sensitive to the stepsize of GD. When the gradients and the stepsize are too small or when the rounding precision is too large, this sensitivity may cause issues such as loss of gradients similar to RN or very slow convergence; see, e.g., Figure 9b. On the other hand, SR_ε is less sensitive to the stepsize of GD such that changing t can hardly affect the convergence rate of GD; see Figure 9c. However, when computing GD using SR_ε with a large value of ε , oscillation may happen. When comparing the effects of rounding bias in fixed-point and floating-point arithmetic, the implementation of GD using SR_ε with low-precision floating-point computation behaves similar to a gradient descent method with adaptive stepsizes in each coordinate of the current iterate, whereas the implementation using SR_ε with low-precision fixed-point computation performs similarly to a strategy that combines vanilla gradient descent and stochastic sign gradient descent methods. For most of the numerical studies, SR_ε results in faster convergence of GD in floating-point arithmetic than in fixed-point arithmetic; nevertheless, when training a fully connected NN the convergence of GD with SR_ε in fixed-point arithmetic is fairly similar to that in floating-point arithmetic.

7 Conclusion

We have studied the convergence of the gradient descent method (GD) in limited-precision fixed-point arithmetic using unbiased stochastic rounding (SR) and ε -biased stochastic rounding (SR_ε), for problems satisfying the Polyak–Lojasiewicz condition. In the analysis, we have proven that a linear convergence rate of GD can be obtained when utilizing either SR or SR_ε , and the convergence bound for SR_ε is shown to be stricter than the one corresponding to SR. By delving into the factors that impact the convergence of GD in low-precision computation, we have provided valuable insights and knowledge to guide informed decision-making when selecting an appropriate rounding method for training neural networks (NNs).

In our numerical studies, we have demonstrated that SR_ε provides faster convergence than SR and RN, on average, when the same number format is used. In particular, SR_ε may considerably accelerate the convergence of GD with low-precision computation for both the training of logistic regression models and NNs, and this is potentially valuable for machine learning. The comparison between floating-point and fixed-point computations illustrates that the implementation of GD using SR_ε with floating-point arithmetic performs similarly to a gradient descent method with adaptive stepsizes in each coordinate of the current iterate, while the implementation using SR_ε with fixed-point arithmetic behaves like a combination of vanilla gradient descent and stochastic sign gradient descent methods. For the training of a fully connected NN, the convergence of GD with SR_ε in fixed-point arithmetic is very similar to that in floating-point arithmetic, and for both number formats, the performance of GD using SR_ε is superior to that of SR.

Acknowledgement

We thank the reviewers for their constructive comments and the editors for the handling of this paper. We thank Mark Peletier for discussions on the upper bound on the PL constant.

Declarations

Funding This research was funded by the EU ECSEL Joint Undertaking under grant agreement no. 826452 (project Arrowhead Tools).

Data availability The MNIST dataset used in this study is available in the open repository https://git-disl.github.io/GTDLBench/datasets/mnist_datasets/.

Conflict of interest The authors declare that they have no conflict of interest.

Appendix A Proofs of lemmas

In this appendix, we prove some helpful lemmas used in our convergence analysis.

Proof of Lemma 3. Under the condition of Case I (15), we consider the upper bound and lower bound of $r_i^{(k)}$ in two scenarios, i.e., $t|\nabla f(\tilde{\mathbf{x}}^{(k)})_i + \sigma_{1,i}^{(k)}| = u$ (S1) and $t|\nabla f(\tilde{\mathbf{x}}^{(k)})_i + \sigma_{1,i}^{(k)}| > u$ (S2).

S1: The condition $t|\nabla f(\tilde{\mathbf{x}}^{(k)})_i + \sigma_{1,i}^{(k)}| = u$ implies that $\sigma_{2,i}^{(k)} = 0$, which results in $r_i^{(k)} = \frac{\sigma_{1,i}^{(k)}}{\nabla f(\tilde{\mathbf{x}}^{(k)})_i}$. Condition (15) implies that $\nabla f(\tilde{\mathbf{x}}^{(k)})_i \neq -\sigma_{1,i}^{(k)}$, i.e., $r_i^{(k)} \neq -1$, and (14) gives $-1 \leq r_i^{(k)} \leq 1$. Therefore, we have that $-1 < r_i^{(k)} \leq 1$ under conditions (14) and (15).

S2: When $t|\nabla f(\tilde{\mathbf{x}}^{(k)})_i + \sigma_{1,i}^{(k)}| > u$, observing that $\sigma_{2,i}^{(k)} < u$, we have $r_i^{(k)} = \frac{t\sigma_{1,i}^{(k)} + \sigma_{2,i}^{(k)}}{t\nabla f(\tilde{\mathbf{x}}^{(k)})_i} < \frac{t\sigma_{1,i}^{(k)} + t|\nabla f(\tilde{\mathbf{x}}^{(k)})_i + \sigma_{1,i}^{(k)}|}{t\nabla f(\tilde{\mathbf{x}}^{(k)})_i} \leq 3$. Concerning the lower bound we consider separately the cases where $\sigma_{1,i}^{(k)}$ and $\nabla f(\tilde{\mathbf{x}}^{(k)})_i$ have the same or opposite signs. When $\text{sign}(\sigma_{1,i}) = \text{sign}(\nabla f(\tilde{\mathbf{x}}^{(k)})_i)$ we have that

$$r_i^{(k)} \geq \frac{|t\sigma_{1,i}| - |\sigma_{2,i}|}{|t\nabla f(\tilde{\mathbf{x}}^{(k)})_i|} > \frac{|t\sigma_{1,i}| - |t\nabla f(\tilde{\mathbf{x}}^{(k)})_i + t\sigma_{1,i}|}{|t\nabla f(\tilde{\mathbf{x}}^{(k)})_i|} = -1.$$

When $\text{sign}(\sigma_{1,i}) = -\text{sign}(\nabla f(\tilde{\mathbf{x}}^{(k)})_i)$, (14) and the property $t|\nabla f(\tilde{\mathbf{x}}^{(k)})_i + \sigma_{1,i}^{(k)}| > u$ yield $|t\nabla f(\tilde{\mathbf{x}}^{(k)})_i| - |t\sigma_{1,i}^{(k)}| > u$, which implies $\frac{-|t\sigma_{1,i}^{(k)}|}{|t\nabla f(\tilde{\mathbf{x}}^{(k)})_i|} > -1 + \frac{u}{|t\nabla f(\tilde{\mathbf{x}}^{(k)})_i|}$. Therefore, we have

$$r_i^{(k)} \geq \frac{-|t\sigma_{1,i}^{(k)}| - |\sigma_{2,i}^{(k)}|}{|t\nabla f(\tilde{\mathbf{x}}^{(k)})_i|} > -1 + \frac{u - |\sigma_{2,i}^{(k)}|}{|t\nabla f(\tilde{\mathbf{x}}^{(k)})_i|} \geq -1.$$

Combining these two scenarios, we have $-1 < r_i^{(k)} < 3$ concluding the proof. \square

Proof of Lemma 4. Clearly, we have

$$\mathbb{E}[\nabla f(\tilde{\mathbf{x}}^{(k)})^T (\nabla f(\tilde{\mathbf{x}}^{(k)}) + \boldsymbol{\sigma}_1^{(k)})] = \mathbb{E}[\|\nabla f(\tilde{\mathbf{x}}^{(k)})\|^2] + \sum_{i=1}^n \mathbb{E}[\sigma_{1,i}^{(k)} \nabla f(\tilde{\mathbf{x}}^{(k)})_i].$$

The second condition in Assumption 1 implies $\mathbb{E}[\sigma_{1,i}^{(k)} \mid \nabla f(\tilde{\mathbf{x}}^{(k)})_i] \lesssim c u^2$ and based on the law of total expectation, we obtain

$$\begin{aligned} |\mathbb{E}[\sigma_{1,i}^{(k)} \nabla f(\tilde{\mathbf{x}}^{(k)})_i]| &= \left| \sum_{\nabla f(\tilde{\mathbf{x}}^{(k)})_i = q} \mathbb{E}[\sigma_{1,i}^{(k)} \nabla f(\tilde{\mathbf{x}}^{(k)})_i \mid \nabla f(\tilde{\mathbf{x}}^{(k)})_i = q] P(\nabla f(\tilde{\mathbf{x}}^{(k)})_i = q) \right| \\ &\lesssim \sum_{\nabla f(\tilde{\mathbf{x}}^{(k)})_i = q} c u^2 |q| P(\nabla f(\tilde{\mathbf{x}}^{(k)})_i = q) \\ &= c u^2 \mathbb{E}[|\nabla f(\tilde{\mathbf{x}}^{(k)})_i|], \end{aligned}$$

which in turn yields that $\sum_{i=1}^n \mathbb{E}[\sigma_{1,i}^{(k)} \nabla f(\tilde{\mathbf{x}}^{(k)})_i]$ is bounded from above by

$$c u^2 \mathbb{E}[\|\nabla f(\tilde{\mathbf{x}}^{(k)})\|_1] \leq \sqrt{n} c u^2 \mathbb{E}[\|\nabla f(\tilde{\mathbf{x}}^{(k)})\|] \leq L \chi \sqrt{n} c u^2.$$

□

Proof of Lemma 6. When SR_ε is applied, on the basis of (6) and (8), we have

$$\begin{aligned} &\mathbb{E}[\sigma_{2,i}^{(k)} \mid t(\nabla f(\tilde{\mathbf{x}}^{(k)})_i + \sigma_{1,i}^{(k)})] \\ &= \begin{cases} \varepsilon u \text{sign}(\nabla f(\tilde{\mathbf{x}}^{(k)})_i + \sigma_{1,i}^{(k)}), & 0 < p_\varepsilon < 1, \\ \lfloor t(\nabla f(\tilde{\mathbf{x}}^{(k)})_i + \sigma_{1,i}^{(k)}) \rfloor - t(\nabla f(\tilde{\mathbf{x}}^{(k)})_i + \sigma_{1,i}^{(k)}) + u, & p_\varepsilon = 0, \\ \lfloor t(\nabla f(\tilde{\mathbf{x}}^{(k)})_i + \sigma_{1,i}^{(k)}) \rfloor - t(\nabla f(\tilde{\mathbf{x}}^{(k)})_i + \sigma_{1,i}^{(k)}), & p_\varepsilon = 1. \end{cases} \quad (\text{A1}) \end{aligned}$$

Note that we omit the dependency on $t(\nabla f(\tilde{\mathbf{x}}^{(k)})_i + \sigma_{1,i}^{(k)})$ in p_ε for brevity. Furthermore, $p_\varepsilon(t(\nabla f(\tilde{\mathbf{x}}^{(k)})_i + \sigma_{1,i}^{(k)})) = 0$ implies $\nabla f(\tilde{\mathbf{x}}^{(k)})_i + \sigma_{1,i}^{(k)} > 0$ and $p_\varepsilon(t(\nabla f(\tilde{\mathbf{x}}^{(k)})_i + \sigma_{1,i}^{(k)})) = 1$ implies $\nabla f(\tilde{\mathbf{x}}^{(k)})_i + \sigma_{1,i}^{(k)} < 0$; on the basis of (14), we have $\text{sign}(\nabla f(\tilde{\mathbf{x}}^{(k)})_i + \sigma_{1,i}^{(k)}) = \text{sign}(\nabla f(\tilde{\mathbf{x}}^{(k)})_i)$. Therefore, we have

$$\begin{aligned} &\mathbb{E}[\sigma_{2,i}^{(k)} \nabla f(\tilde{\mathbf{x}}^{(k)})_i \mid t(\nabla f(\tilde{\mathbf{x}}^{(k)})_i + \sigma_{1,i}^{(k)})] \quad (\text{A2}) \\ &= \begin{cases} \varepsilon u |\nabla f(\tilde{\mathbf{x}}^{(k)})_i|, & 0 < p_\varepsilon < 1, \\ \lfloor t(\nabla f(\tilde{\mathbf{x}}^{(k)})_i + \sigma_{1,i}^{(k)}) \rfloor - t(\nabla f(\tilde{\mathbf{x}}^{(k)})_i + \sigma_{1,i}^{(k)}) + u |\nabla f(\tilde{\mathbf{x}}^{(k)})_i|, & p_\varepsilon = 0, \\ \lfloor t(\nabla f(\tilde{\mathbf{x}}^{(k)})_i + \sigma_{1,i}^{(k)}) \rfloor - t(\nabla f(\tilde{\mathbf{x}}^{(k)})_i + \sigma_{1,i}^{(k)}) |\nabla f(\tilde{\mathbf{x}}^{(k)})_i|, & p_\varepsilon = 1, \end{cases} \end{aligned}$$

which are all positive random variables for all the three cases, concluding the claim. □

Proof of Lemma 8.. We denote by \mathcal{S} the finite set of values that the i th component of $\nabla f(\tilde{\mathbf{x}}^{(k)}) + \sigma_1^{(k)}$ can assume. The set \mathcal{S}_1 is the subset of \mathcal{S} such that for all $\nabla f(\tilde{\mathbf{x}}^{(k)})_i + \sigma_{1,i}^{(k)} \in \mathcal{S}_1$ satisfying $0 < p_\varepsilon(t(\nabla f(\tilde{\mathbf{x}}^{(k)})_i + \sigma_i^{(k)})) < 1$. Analogously we define \mathcal{S}_2 and \mathcal{S}_3 associated with the conditions $p_\varepsilon = 0$ and $p_\varepsilon = 1$, respectively. According to the law of total expectation, we have

$$\mathbb{E}[\sigma_{2,i}^{(k)} \nabla f(\tilde{\mathbf{x}}^{(k)})_i] = \sum_{j=1,2,3} \mathbb{E}[\sigma_{2,i}^{(k)} \nabla f(\tilde{\mathbf{x}}^{(k)})_i \mid f(\tilde{\mathbf{x}}^{(k)})_i + \sigma_i^{(k)} \in \mathcal{S}_j] P(f(\tilde{\mathbf{x}}^{(k)})_i + \sigma_i^{(k)} \in \mathcal{S}_j).$$

Note that in view of (8b), we have

$$p_\varepsilon = 1 \quad \Rightarrow \quad |[t(\nabla f(\tilde{\mathbf{x}}^{(k)})_i + \sigma_{1,i}^{(k)})] - t(\nabla f(\tilde{\mathbf{x}}^{(k)})_i + \sigma_{1,i}^{(k)})| < \varepsilon u$$

and

$$p_\varepsilon = 0 \quad \Rightarrow \quad |[t(\nabla f(\tilde{\mathbf{x}}^{(k)})_i + \sigma_{1,i}^{(k)})] - t(\nabla f(\tilde{\mathbf{x}}^{(k)})_i + \sigma_{1,i}^{(k)}) + u| < \varepsilon u.$$

Together with (A1), we obtain $\min_{i=1,\dots,n} \mathbb{E}[\sigma_{2,i}^{(k)} \nabla f(\tilde{\mathbf{x}}^{(k)})_i] \leq \varepsilon u \min_{i=1,\dots,n} \mathbb{E}[|\nabla f(\tilde{\mathbf{x}}^{(k)})_i|]$. Jensen's inequality gives that $\sqrt{n} \min_{i=1,\dots,n} \mathbb{E}[|\nabla f(\tilde{\mathbf{x}}^{(k)})_i|] \leq \mathbb{E}[\|\nabla f(\tilde{\mathbf{x}}^{(k)})\|]$; together with condition (22), we have

$$\begin{aligned} \rho_k &= \min_{i=1,\dots,n} \frac{n \mathbb{E}[\sigma_{2,i}^{(k)} \nabla f(\tilde{\mathbf{x}}^{(k)})_i]}{\mathbb{E}[\|\nabla f(\tilde{\mathbf{x}}^{(k)})\|^2]} \leq \frac{n \varepsilon u \min_{i=1,\dots,n} \mathbb{E}[|\nabla f(\tilde{\mathbf{x}}^{(k)})_i|]}{\mathbb{E}[\|\nabla f(\tilde{\mathbf{x}}^{(k)})\|^2]} \\ &\leq \frac{\sqrt{n} u \varepsilon \mathbb{E}[\|\nabla f(\tilde{\mathbf{x}}^{(k)})\|]}{\mathbb{E}[\|\nabla f(\tilde{\mathbf{x}}^{(k)})\|^2]} \stackrel{(22)}{\leq} \frac{2t\varepsilon \mathbb{E}[\|\nabla f(\tilde{\mathbf{x}}^{(k)})\|^2]}{\mathbb{E}[\|\nabla f(\tilde{\mathbf{x}}^{(k)})\|^2]}, \end{aligned}$$

which leads to $\rho_k \leq 2t\varepsilon$, according to Jensen's inequality. Conditions (14) and (15) imply that $|\nabla f(\tilde{\mathbf{x}}^{(k)})_i| > 0$. Together with (A2), we have $0 < \rho_k \leq 2t\varepsilon$. \square

Appendix B Proofs of propositions

Proof of Proposition 16. When $\sigma_{1,i}^{(k)}$ and $\sigma_{2,i}^{(k)}$ are obtained by SR and SR_ε , respectively, substituting (29) and (45) into (49) yields

$$\begin{aligned} \mathbb{E}[f(\tilde{\mathbf{x}}^{(k+1)})] &\lesssim \mathbb{E}[f(\tilde{\mathbf{x}}^{(k)})] - \frac{1}{2} \sum_{i \in \mathcal{C}_1} (t \mathbb{E}[\nabla f(\tilde{\mathbf{x}}^{(k)})_i^2] + \mathbb{E}[\sigma_{2,i}^k \nabla f(\tilde{\mathbf{x}}^{(k)})_i]) \\ &\quad - \frac{1}{2} \theta_k \sum_{i \in \mathcal{C}_2} (t \mathbb{E}[\nabla f(\tilde{\mathbf{x}}^{(k)})_i^2] + \beta_k u \mathbb{E}[|\nabla f(\tilde{\mathbf{x}}^{(k)})_i|]) \\ &= \mathbb{E}[f(\tilde{\mathbf{x}}^{(k)})] - \frac{1}{2} t \mathbb{E}[\|\nabla f(\tilde{\mathbf{x}}^{(k)})\|^2] \\ &\quad - \sum_{i \in \mathcal{C}_1} (\mathbb{E}[\sigma_{2,i}^k \nabla f(\tilde{\mathbf{x}}^{(k)})_i] - \frac{1}{2} \theta_k \beta_k u \mathbb{E}[|\nabla f(\tilde{\mathbf{x}}^{(k)})_i|]) \\ &\quad - \sum_{i \in \mathcal{C}_2} \frac{1}{2} (\theta_k - 1) t \mathbb{E}[\nabla f(\tilde{\mathbf{x}}^{(k)})_i^2] - \frac{1}{2} \theta_k \beta_k u \mathbb{E}[\|\nabla f(\tilde{\mathbf{x}}^{(k)})\|]. \end{aligned}$$

Furthermore, the properties $\beta_k u \leq |\mathbb{E}[\sigma_{2,i}^{(k)}]|$ and $\theta_k \leq 2$ imply that $\frac{1}{2} \beta_k u \mathbb{E}[|\nabla f(\tilde{\mathbf{x}}^{(k)})_i|] \leq \mathbb{E}[\sigma_{2,i}^{(k)} \nabla f(\tilde{\mathbf{x}}^{(k)})_i]$. On the basis of (43) and (47), we have

$$\mathbb{E}[f(\tilde{\mathbf{x}}^{(k+1)})] \lesssim \mathbb{E}[f(\tilde{\mathbf{x}}^{(k)})] - \frac{1}{2} (t + \theta_k \tau_2 + \alpha_k) \mathbb{E}[\|\nabla f(\tilde{\mathbf{x}}^{(k)})\|^2].$$

Expanding the recursion k times, we obtain (51), with $\tau_2 < 2t\varepsilon$ and $|\alpha_j| < t|\theta_j - 1|$ for all j . Since $\mu(t + \alpha_j + \theta_j \tau_2) \leq \mu t(1 + |\theta_j - 1| + 2\theta_j \varepsilon) \leq \mu t(1 + 1 + 4\varepsilon) \leq 2\mu t(1 + 2\varepsilon) \leq Lt(1 + 2\varepsilon) \leq \frac{1+2\varepsilon}{4} < 1$. Further the property $1 - 2\mu t > 0$ and $-t < \alpha_j < t$ (cf. (47)) indicate that $1 - \mu(t + \alpha_j) > 1 - 2\mu t > 0$, combining with the property $\theta_j \tau_2 > 0$ we have $0 \leq \mu(t + \alpha_j + \theta_j \tau_2) < 1$. \square

Proof of Proposition 17. The unbiased property of SR yields (53). According to (8a) and (53), for $\nabla f(\mathbf{x}^{(k)})_i < 0$, we have $-u p_0(t \nabla f(\mathbf{x}^{(k)})_i) = t \nabla f(\mathbf{x}^{(k)})_i$, which indicates

$$\begin{aligned} -u p_\varepsilon(t \nabla f(\mathbf{x}^{(k)})_i) &= -u (p_0(t \nabla f(\mathbf{x}^{(k)})_i) + \text{sign}(\nabla f(\mathbf{x}^{(k)})_i) \varepsilon) \\ &= t \nabla f(\mathbf{x}^{(k)})_i + \varepsilon u \text{sign}(\nabla f(\mathbf{x}^{(k)})_i). \end{aligned}$$

The same result can be obtained for $\nabla f(\mathbf{x}^{(k)})_i > 0$ by using the property $t \nabla f(\mathbf{x}^{(k)})_i = u(1 - p_0(t \nabla f(\tilde{\mathbf{x}}^{(k)})_i))$. \square

Proof of Proposition 18. Derived from the model of floating-point number representation [19, Sec. 2.3], we have

$$\text{fl}(x_i^{(k)} - t \nabla f(\mathbf{x}^{(k)})_i) = \begin{cases} (x_i^{(k)} - t \nabla f(\mathbf{x}^{(k)})_i) (1 + \delta_i^{(k)}), & \text{if } \text{sign}(x_i^{(k)} \nabla f(\mathbf{x}^{(k)})_i) = -1, \\ (x_i^{(k)} - t \nabla f(\mathbf{x}^{(k)})_i) (1 - \delta_i^{(k)}), & \text{if } \text{sign}(x_i^{(k)} \nabla f(\mathbf{x}^{(k)})_i) = 1, \end{cases}$$

where $0 < \delta_i^{(k)} < 2u$. In light of (13), we obtain

$$\begin{aligned} \tilde{d}_i^{(k)} &= x_i^{(k)} - \text{fl}(x_i^{(k)} - t \nabla f(\mathbf{x}^{(k)})_i) \\ &= \begin{cases} -\delta_i^{(k)} x_i^{(k)} + t \nabla f(\mathbf{x}^{(k)})_i (1 + \delta_i^{(k)}), & \text{if } \text{sign}(x_i^{(k)} \nabla f(\mathbf{x}^{(k)})_i) = -1, \\ \delta_i^{(k)} x_i^{(k)} + t \nabla f(\mathbf{x}^{(k)})_i (1 - \delta_i^{(k)}), & \text{if } \text{sign}(x_i^{(k)} \nabla f(\mathbf{x}^{(k)})_i) = 1. \end{cases} \end{aligned}$$

On the basis of the unbiased property of SR and taking the expectation of $\tilde{d}_i^{(k)}$, we obtain $\mathbb{E}[\tilde{d}_i^{(k)} \mid x_i^{(k)} - t \nabla f(\mathbf{x}^{(k)})_i] = t \nabla f(\mathbf{x}^{(k)})_i$, which gives (54). On the basis of (54) and (9), by making $\text{sign}(v) = \text{sign}(\nabla f(\mathbf{x}^{(k)})_i)$ in signed-SR $_\varepsilon$ (cf. (9)), when $x_i^{(k)} > 0$ and $\nabla f(\tilde{\mathbf{x}}^{(k)})_i < 0$, we have

$$\begin{aligned} \mathbb{E}[\tilde{d}_i^{(k)} \mid x_i^{(k)} - t \nabla f(\mathbf{x}^{(k)})_i] &= (-\delta_i^{(k)} x_i^{(k)} + t \nabla f(\mathbf{x}^{(k)})_i (1 + \delta_i^{(k)})) (1 - p_0(x_i^{(k)} - t \nabla f(\mathbf{x}^{(k)})_i) - \text{sign}(\nabla f(\mathbf{x}^{(k)})_i) \varepsilon) \\ &= t \nabla f(\mathbf{x}^{(k)})_i + \varepsilon (-\delta_i^{(k)} x_i^{(k)} + t \nabla f(\mathbf{x}^{(k)})_i (1 + \delta_i^{(k)})) \\ &= (1 + \varepsilon + \varepsilon \delta_i^{(k)}) t \nabla f(\mathbf{x}^{(k)})_i + \text{sign}(\nabla f(\mathbf{x}^{(k)})_i) |x_i^{(k)}| \varepsilon \delta_i^{(k)}. \end{aligned}$$

Analogously, when $x_i^{(k)} < 0$ and $\nabla f(\mathbf{x}^{(k)})_i > 0$, we have

$$\begin{aligned} & \mathbb{E}[\tilde{d}_i^{(k)} \mid x_i^{(k)} - t \nabla f(\mathbf{x}^{(k)})_i] \\ &= (-\delta_i^{(k)} x_i^{(k)} + t \nabla f(\mathbf{x}^{(k)})_i (1 + \delta_i^{(k)})) (p_0(x_i^{(k)} - t \nabla f(\mathbf{x}^{(k)})_i) + \text{sign}(\nabla f(\mathbf{x}^{(k)})_i) \varepsilon) \\ &= (1 + \varepsilon + \varepsilon \delta_i^{(k)}) t \nabla f(\mathbf{x}^{(k)})_i + \text{sign}(\nabla f(\mathbf{x}^{(k)})_i) |x_i^{(k)}| \varepsilon \delta_i^{(k)}. \end{aligned}$$

Therefore, (55) holds for the case when $\text{sign}(x_i^{(k)} \nabla f(\mathbf{x}^{(k)})_i) = -1$. The proof of (55) for the case when $\text{sign}(x_i^{(k)} \nabla f(\mathbf{x}^{(k)})_i) = 1$ can be obtained by an analogous argument as the one for $\text{sign}(x_i^{(k)} \nabla f(\mathbf{x}^{(k)})_i) = -1$. \square

References

- [1] Wang, N., Choi, J., Brand, D., Chen, C.-Y., Gopalakrishnan, K.: Training deep neural networks with 8-bit floating point numbers. In: Proc. 32nd Conf. Neural Inf. Process. Syst., pp. 7675–7684 (2018)
- [2] Gupta, S., Agrawal, A., Gopalakrishnan, K., Narayanan, P.: Deep learning with limited numerical precision. In: Proc. 32nd Int. Conf. Mach. Learn., pp. 1737–1746 (2015)
- [3] Chen, X., Hu, X., Zhou, H., Xu, N.: FxpNet: Training a deep convolutional neural network in fixed-point representation. In: 2017 International Joint Conference on Neural Networks, IEEE, pp. 2494–2501 (2017)
- [4] Palossi, D., Zimmerman, N., Burrello, A., Conti, F., Müller, H., Gambardella, L.M., Benini, L., Giusti, A., Guzzi, J.: Fully onboard AI-powered human-drone pose estimation on ultralow-power autonomous flying nano-UAVs. *IEEE Internet Things J.* **9**(3), 1913–1929 (2021)
- [5] Müller, H., Palossi, D., Mach, S., Conti, F., Benini, L.: Fünfiber-drone: A modular open-platform 18-grams autonomous nano-drone. In: 2021 Design, Automation & Test in Europe Conference & Exhibition, IEEE, pp. 1610–1615 (2021)
- [6] Niculescu, V., Lamberti, L., Conti, F., Benini, L., Palossi, D.: Improving autonomous nano-drones performance via automated end-to-end optimization and deployment of DNNs. *IEEE J. Emerg. Sel. Top. Circuits Syst.* **11**(4), 548–562 (2021)
- [7] Nesterov, Y.: *Introductory Lectures on Convex Optimization: A Basic Course*. Springer, New York, US (2003)
- [8] Polyak, B.T.: Gradient methods for solving equations and inequalities. *USSR Comput. Math. & Math. Phys.* **4**(6), 17–32 (1963)

- [9] Lojasiewicz, S.: A topological property of real analytic subsets. *Coll. du CNRS, Les équations aux dérivées partielles* **117**, 87–89 (1963)
- [10] Karimi, H., Nutini, J., Schmidt, M.: Linear convergence of gradient and proximal-gradient methods under the Polyak-Lojasiewicz condition. In: *Proc. Mach. Learn. Knowl. Discovery in Databases: Eur. Conf.*, Springer, pp. 795–811 (2016)
- [11] Charles, Z., Papailiopoulos, D.: Stability and generalization of learning algorithms that converge to global optima. In: *Int. Conf. Mach. Learn.*, PMLR, pp. 745–754 (2018)
- [12] Nguyen, Q.N., Mondelli, M.: Global convergence of deep networks with one wide layer followed by pyramidal topology. In: *Proc. 34th Conf. Neural Inf. Process. Syst.*, pp. 11961–11972 (2020)
- [13] Frei, S., Gu, Q.: Proxy convexity: A unified framework for the analysis of neural networks trained by gradient descent. In: *Proc. 35th Conf. Neural Inf. Process. Syst.*, pp. 7937–7949 (2021)
- [14] Liu, C., Zhu, L., Belkin, M.: Loss landscapes and optimization in over-parameterized non-linear systems and neural networks. *Appl. Comput. Harmon. Anal.* (2022)
- [15] Higham, N.J.: *Accuracy and Stability of Numerical Algorithms*. SIAM, Philadelphia, US (2002)
- [16] Connolly, M.P., Higham, N.J., Mary, T.: Stochastic rounding and its probabilistic backward error analysis. *SIAM J. Sci. Comput.* **43**(1), 566–585 (2021)
- [17] Na, T., Ko, J.H., Kung, J., Mukhopadhyay, S.: On-chip training of recurrent neural networks with limited numerical precision. In: *Proc. Int. Jt. Conf. Neural Netw.*, IEEE, pp. 3716–3723 (2017)
- [18] Ortiz, M., Cristal, A., Ayguadé, E., Casas, M.: Low-precision floating-point schemes for neural network training. *arXiv: 1804.05267* (2018)
- [19] Xia, L., Massei, S., Hochstenbach, M.E., Koren, B.: On stochastic roundoff errors in gradient descent with low-precision computation. *J. Optim. Theory Appl.* **200**(2), 634–668 (2024)
- [20] Oberstar, E.L.: *Fixed-point representation & fractional math*. Oberstar Consulting **9** (2007)
- [21] Santoro, M.R., Bewick, G., Horowitz, M.A.: Rounding algorithms for IEEE multipliers. In: *Proc. 9th Symp. Comput. Arithmetic*, IEEE, pp. 176–183 (1989)
- [22] Yates, R.: Fixed-point arithmetic: An introduction. *Digital Signal Labs* **81**(83), 198 (2009)

- [23] Linnainmaa, S.: Taylor expansion of the accumulated rounding error. *BIT Numer. Math.* **16**(2), 146–160 (1976)
- [24] Boyd, S., Vandenberghe, L.: *Convex Optimization*. Cambridge University Press, Cambridge, UK (2004)
- [25] Polyak, B.T.: Some methods of speeding up the convergence of iteration methods. *USSR Comput. Math. & Math. Phys.* **4**(5), 1–17 (1964)
- [26] Bertsekas, D.P., Tsitsiklis, J.N.: Gradient convergence in gradient methods with errors. *SIAM J. Optim.* **10**(3), 627–642 (2000)
- [27] Schmidt, M., Roux, N., Bach, F.: Convergence rates of inexact proximal-gradient methods for convex optimization. In: *Proc. of the 24th Neural Inf. Process. Syst. Conf.*, pp. 1458–1466 (2011)
- [28] Nguyen, L.M., Nguyen, N.H., Phan, D.T., Kalagnanam, J.R., Scheinberg, K.: When does stochastic gradient algorithm work well? *arXiv:1801.06159* (2018)
- [29] NVIDIA, Train with Mixed Precision. Available at <https://docs.nvidia.com/deeplearning/performance/pdf/Training-Mixed-Precision-User-Guide.pdf> (2023)
- [30] Moulay, E., Léchappé, V., Plestan, F.: Properties of the sign gradient descent algorithms. *Inf. Sci.* **492**, 29–39 (2019)
- [31] Biagini, F., Campanino, M.: *Elements of Probability and Statistics*. Springer, Cham, Switzerland (2016)
- [32] Steyer, R., Nagel, W.: *Probability and Conditional Expectation: Fundamentals for the Empirical Sciences*. John Wiley & Sons, Chichester, UK (2017)
- [33] Chen, J., Tsai, C.-A., Moon, H., Ahn, H., Young, J., Chen, C.-H.: Decision threshold adjustment in class prediction. *SAR QSAR Environ. Res.* **17**(3), 337–352 (2006)
- [34] Glorot, X., Bengio, Y.: Understanding the difficulty of training deep feedforward neural networks. In: *Proc. 13th Int. Conf. Artif. Intell. Stat.*, pp. 249–256 (2010)